European Journal of Medicinal Chemistry 101 (2015) 560–572

Contents lists available at ScienceDirect

European Journal of Medicinal Chemistry

journal homepage: http://www.elsevier.com/locate/ejmech

Research paper

Reversal of P-gp and BCRP-mediated MDR by tariquidar derivatives

Xu-Qin Li [a, *, 1], Lin Wang [b, 1], Yan Lei [a], Tao Hu [b], Fei-Long Zhang [a], Chi-Hin Cho [b], Kenneth K.W. To [c, **]

[a] Department of Chemistry, University of Science and Technology Beijing, No. 30 Xueyuan Road, Haidian District, Beijing 100083, China
[b] School of Biomedical Sciences, Faculty of Medicine, The Chinese University of Hong Kong, Hong Kong Special Administrative Region
[c] School of Pharmacy, Faculty of Medicine, The Chinese University of Hong Kong, Hong Kong Special Administrative Region

ARTICLE INFO

Article history:
Received 29 April 2015
Received in revised form
24 June 2015
Accepted 27 June 2015
Available online 10 July 2015

Keywords:
Multidrug resistance
P-Glycoprotein
Breast cancer resistance protein
Sulfonamide
Anthranilamide

ABSTRACT

With an aim to generate non-toxic, specific and highly potent multidrug resistance (MDR) modulators, a novel series of anthranilic acid amide-substituted tariquidar derivatives were synthesized. The new compounds were evaluated for their cytotoxicity toward normal human colon fibroblasts (CCD18-Co), human gastric epithelial cell line (HFE) and primary rat liver cells, and for their ability to inhibit P-gp/BCRP-mediated drug efflux and reversal of P-gp and BCRP-mediated MDR in parental and drug-resistant cancer cell lines (LCC6 MDR1, MCF-7 FLV1000, R-HepG2, SW620-Ad300). While tariquidar is highly toxic to normal cells, the new derivatives exhibited much lower or negligible cytotoxicity. Some of the new tariquidar derivatives inhibited both P-gp and BCRP-mediated drug efflux whereas a few of them bearing a sulfonamide functional group (**1**, **5**, and **16**) are specific to P-gp. The new compounds were also found to potentiate the anticancer activity of the transporter substrate anticancer drugs in the corresponding transporter-overexpressing cell lines. The extent of resistance reversal was found to be consistent with the transporter inhibitory effect of the new derivatives. To further understand the mechanism of P-gp and BCRP inhibition, the tariquidar derivatives were found to interact with the transporters using an antibody-based UIC2 or 5D3 shift assay. Moreover, the transporters-inhibiting derivatives were found to modulate the ATPase activities of the two MDR transporters. Our data thus advocate further development of the new compounds for the circumvention of MDR.

1. Introduction

Multidrug resistance (MDR) in cancer chemotherapy is the major cause of treatment failure in over 90% of patients with metastatic cancer [1]. While MDR can be mediated by various mechanisms, the over-expression of the ATP-binding cassette (ABC) transporters that actively pump drugs out of the cell is commonly considered the most important contributor to drug resistance. A logical strategy to circumvent MDR is therefore the development of efficient inhibitors for these ABC transporters. Among these transporters, the most extensively studied ones are P-glycoprotein (P-gp, encoded by the gene *ABCB1*), multidrug resistance-associated protein 1 (MRP1, encoded by the gene *ABCC1*), and breast cancer resistance protein (BCRP, encoded by the gene *ABCG2*) [2]. Due to the importance of these MDR transporters in clinical oncology, there has been an intense search for effective inhibitors of especially P-gp and ABCG2. Three generation of P-gp inhibitors have been developed to date. Verapamil is the first known P-gp ligand reported to increase the intracellular concentration of anticancer agents in multidrug resistant cells by inhibiting the P-gp-mediated efflux [3]. This observation fueled hopes that anticancer drug resistance could be reversed by inhibiting drug efflux. To improve the chemotherapy of multidrug-resistant tumors, a range of second generation P-gp inhibitors has been developed from clinically used drugs [4]. However, these drugs were only weak P-

Abbreviations: P-gp, P-glycoprotein; MRP, multidrug resistance associated protein; BCRP, breast cancer resistance protein; MDR, multidrug resistance; ATP, adenosine triphosphate; ABC, ATP binding cassette; QSAR, quantitative structure–activity relationships; HB, hydrogen bond; Rh123, Rhodamine 123; PhA, pheophorbide A; ESI-MS, electrospray ionization mass spectrometry; DCM, dichloromethane; DMF, dimethylformamide; DMSO, dimethylsulfoxide; TLC, thin layer chromatography; EDTA, ethylene diamine tetraacetic acid; DTT, 1,4-dithiothreitol.

* Corresponding author.
** Corresponding author.
E-mail addresses: lixuqin@ustb.edu.cn (X.-Q. Li), kennethto@cuhk.edu.hk (K.K.W. To).

[1] These authors contributed equally to this work.

http://dx.doi.org/10.1016/j.ejmech.2015.06.049
0223-5234/

gp inhibitors *in vivo*. Furthermore, many of these P-gp inhibitors were found to inhibit cytochrome P450 and impair drug clearance [5]. The altered drug pharmacokinetic may necessitate decreases in drug dosing to prevent excess toxicity, thus undermining any benefit that would be obtained from having a drug efflux inhibitor. The design of potent MDR inhibitors devoid of other pharmacological activities has thus become a desirable goal to test the MDR reversal hypothesis in the clinics.

The third generation P-gp inhibitors comprised compounds such as tariquidar (XR9576) [6,7] and elacridar (GF120918), with high affinity to P-gp at nanomolar concentrations to produce specific and effective inhibition of P-gp function [8,9]. As a result, with the concomitant treatment with tariquidar, more chemotherapeutic drugs can be accumulated within tumor cells by efflux transporter inhibition, thereby leading to greater cytotoxicity [10]. Tariquidar has been reported to reverse the resistance of doxorubicin, vinblastine, and paclitaxel in advanced breast cancer [11]. However, tariquidar was found to be highly toxic in a phase III clinical trial for non-small cell lung cancer (NSCLC) patients [12]. A clinical trial assessing the efficacy of the combination of paclitaxel/carboplatin/tariquidar was subsequently suspended due to the poor response and toxicity [5]. Despite the safety concern, the potent and effective property of tariquidar makes it a good lead compound in the search for new MDR inhibitors [13]. To this end, tariquidar exhibited less systemic pharmacokinetic interaction than previous P-gp inhibitors from a pharmacodynamic study of docetaxel in combination with tariquidar in patients with lung, ovarian, and cervical cancer [14]. To date, a large number of tariquidar analogs have been synthesized with an aim to optimize the MDR reversal activity of the original structure [13,15–18,22], which allows detailed investigation of structural activity relationship in tariquidar backbone structure.

It has been postulated that tariquidar bind to the same binding site of P-gp as the P-gp substrate Hoechst 33342 [15a]. Based on the structure of Hoechst 33342, it was proposed that the pharmacophore of tariquidar (Fig. 1) consists of (1) an anthranilamide core structure and a tetrahydroisoquinoline moiety (which facilitate hydrogen bond (HB) interaction with the transporter); (2) a phenyl moiety (which provides an essential hydrophobic site for interaction with the transporter); and (3) a quinolinyl substituent (which is believed to bind to an additional site of the transporter). A 3D QSAR analysis of 62 tariquidar analogs has been performed by Labrie et al. [21]. Apart from steric and electrostatic considerations, the presence of HB acceptors was also believed to be an important property of P-gp inhibitors. These results were also consistent with the parameters reported by Globisch et al. [15b].

In this study, we synthesized a new series of tariquidar derivatives and evaluated their activity on P-gp inhibition and MDR reversal. The general structure of the new compounds is shown in Fig. 2. They possess an anthranilic acid amide substituent (in BB1), a 6,7-dimethoxytetrahydroisoquinoline-ethyl-phenylamine substituent (in BB2) and either a sulfonamide or an amide (in BB3). The synthesis of the new P-gp inhibitors has been optimized, and the new compounds were all obtained with high yield. Our goal is to identify compounds with satisfactory specificity and potent inhibitory activity for P-gp. The new compounds were also evaluated for toxicity to sensitive cells.

2. Results and discussion

2.1. Chemistry

Compounds **1**–**25** were synthesized according to the chemical reactions described in Scheme 1. Two methods were used to couple Ar–NH_2 **27** with two different starting materials to yield the intermediate 2-aminobenzamides **30**. In the first method the amine **27** Ar–NH_2 was allowed to react with isatoic anhydride **26** to give 2-aminobenzamides **30** directly. The second method [17–20,22] utilized an appropriately substituted anthranilic acid (o-nitrobenzoylic acid or 6-Nitroveratric acid) **28** to react with an acid chloride. 2-Aminobenzamides **30** was obtained after reduction of the nitro group. Reaction of **30** with appropriate sulfonyl chloride yielded the sulfonated derivatives of anthranilamides **1**–**18**. Acylation of the resulting aromatic amines **30** with different acid yielded the compounds **19**–**25**.

Following the synthetic scheme reported by Labrie et al. [23], our initial reaction approach was to synthesize **30** from isatoic anhydride by a single step. Unfortunately, the yield was only around 50% when the reaction was allowed to reflux with aromatic amine in acetonitrile for 24 h. The yield did not improve even after the reaction time was extended for another 24 h. Therefore, the reaction conditions were further optimized. After we added acetic acid to the reaction mixture, the yield of **30** was increased to 85% in 2 h. The improved reaction was probably due to acid-catalyzed cleavage of the anhydride.

Interestingly, **1** and **5** were obtained as bis-substituted compounds (Table 1). No mono substituted derivative was produced under the same sulfonyl reaction condition even when sulfonyl chloride was added drop-wisely in the reaction.

It is generally believed that a highly effective P-gp inhibitor should be lipophilic and possess a Log *P* value greater than 2.92 to allow hydrophobic and van der Waals interactions with the key binding residues of P-gp [24]. However, hydrophobicity of the third-generation MDR modulators is not the only determinant for their P-gp inhibition. The structure–activity relationship of P-gp inhibition suggested that multiple factors, including steric, electrostatic, hydrophobic, and hydrogen bonding, were all correlated with the inhibitory potency on the transporter [22], thus we attempted to attach different functional groups (including aromatic, heterocyclic or chain structure) in BB3 for structural optimization. Importantly, the introduction of a sulfonamide functional group into the new compounds was found to result in improved aqueous solubility, as well as better solubility in other solvents compared to tariquidar, which facilitated their pharmacological evaluation and further drug formulation development.

2.2. Biological activity

2.2.1. Cytotoxicity of the compounds in normal and cancer cells

Cytotoxicity of the new compounds and tariquidar (as control for comparison) were evaluated in normal human colon fibroblasts and gastric epithelial cells. While tariquidar was found to be highly toxic (IC_{50} = 1.28 μM) in human gastric epithelial cell, all new compounds exhibited negligible or much lower cytotoxic effect in the normal human colon fibroblasts and human gastric epithelial

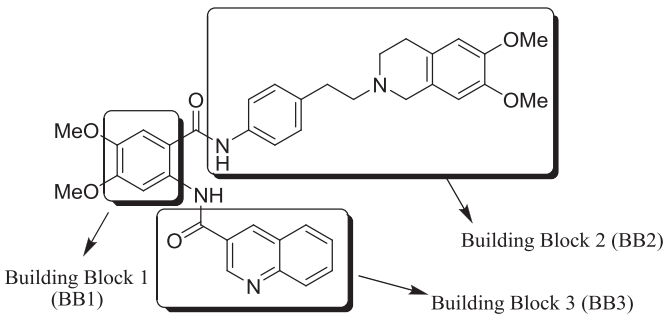

Fig. 1. The three pharmacophores of tariquidar.

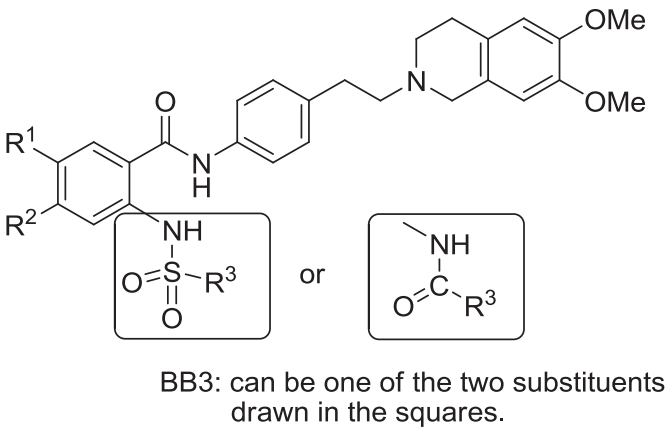

Fig. 2. The general structure of the new compounds.

cells (IC_{50} > 100 μM & IC_{50} > 5 μM, respectively) (Table 2). Similarly, in a panel of three human colon cancer cell lines, while tariquidar exhibited high cytotoxicity, most new compounds were found to have negligible cytotoxicity at concentration <100 μM (Table 2). In addition, when the cytotoxicity of the new compounds and tariquidar were evaluated in primary rat liver cells, similar results were obtained (Supplemental data).

2.2.2. Inhibition of P-gp/BCRP-mediated drug efflux by the new tariquidar derivatives

To understand the mechanism for the reversal of MDR by the tariquidar derivatives, their possible inhibition of P-gp or BCRP transport activity was evaluated. When tested at the concentration of 0.5 μM, **24**, **16**, **5**, **1**, **21**, **23** and **22** were found to specifically inhibit the efflux of Rh123 (a fluorescent P-gp probe substrate) in P-gp transfected K562/P-gp cells to different extent (Fig. 3A). The P-gp efflux inhibition was also found to be concentration dependent (data not shown). No such effect was observed in the backbone vector transfected K562 cells (data not shown). Among the tariquidar derivatives, **24** showed the most potent P-gp inhibitory activity. The activity of **24** was 90.5 ± 4.4% of that of the tariquidar (**25**). When tested at the concentration of 1 μM, **1**, **5**, **11**, **24** were also found to inhibit P-gp mediated efflux of doxorubicin, a clinically widely used fluorescent P-gp substrate drug. **24** also showed the most potent inhibitory activity (Supplemental data). On the other hand, **24**, **21**, **23** and **22** were also found to inhibit BCRP-mediated drug efflux in K562/BCRP cells (Fig. 3B). The BCRP inhibitory effect of **24** and **23** were similar to tariquidar (**25**), whereas **21** and **22** exhibited only ~60% BCRP inhibition compared with tariquidar. Tariquidar is known to inhibit both P-gp and BCRP. We found that the structural modification in **16**, **5** and **1** made them specific only to P-gp. It is reported that tariquidar does not inhibit MRP1 [10]. To evaluate whether the structural modification of tariquidar could change the substrate/inhibitor specificity on MRP1, we also detected the effects of the tariquidar derivatives on MRP1-mediated calcein-AM efflux in the MRP1-stable transfected HEK293 cells. As shown in Supplementary Fig. 27, none of the tariquidar derivatives showed MRP1 inhibitory activity.

2.2.3. Reversal of P-gp and BCRP-mediated MDR by tariquidar derivatives

The reversal of multidrug resistance by the new tariquidar derivatives was evaluated in four pairs of parental and drug-resistant cancer cell lines with overexpression of P-gp or BCRP. The multidrug resistant cancer cell lines are remarkably resistant to the corresponding substrate anticancer drugs (Table 3) (i.e. P-gp-overexpressing LCC6 MDR1: 125-fold resistant to paclitaxel; BCRP-overexpressing MCF-7 FLV1000: 208-fold resistant to mitoxantrone; R-HepG2: 14 fold resistant to doxorubicin, SW620-AD300: 15 fold resistant to doxorubicin). The new tariquidar derivatives, when used at 200 nM, potentiate the anticancer activity of the transporter substrate anticancer drugs in the corresponding transporter-overexpressing cell lines (Table 3). At 200 nM, the new compounds alone did not affect cell proliferation. Moreover, the extent of resistance reversal was found to be consistent with the transporter inhibitory activity of the new derivatives (Fig. 3). Their effects were specific since resistance reversal was not observed in the parental cells.

2.2.4. Increased UIC2 or 5D3 labeling by the effective tariquidar derivatives suggest their interaction with P-gp and BCRP

UIC2 and 5D3 are conformation sensitive monoclonal antibodies, recognizing an extracellular epitope of the human P-gp and BCRP, respectively. UIC2/5D3 binding to an extracellular loop of the transporters was known to be increased in certain conformations of the transporter protein, upon substrate/inhibitor binding and ATP hydrolysis (i.e. UIC2 or 5D3 shift) [25,26]. The UIC2 and 5D3 shift assay were therefore performed in K562/P-gp and K562/BCRP, respectively, to demonstrate the interaction of tariquidar derivatives with these two MDR transporters.

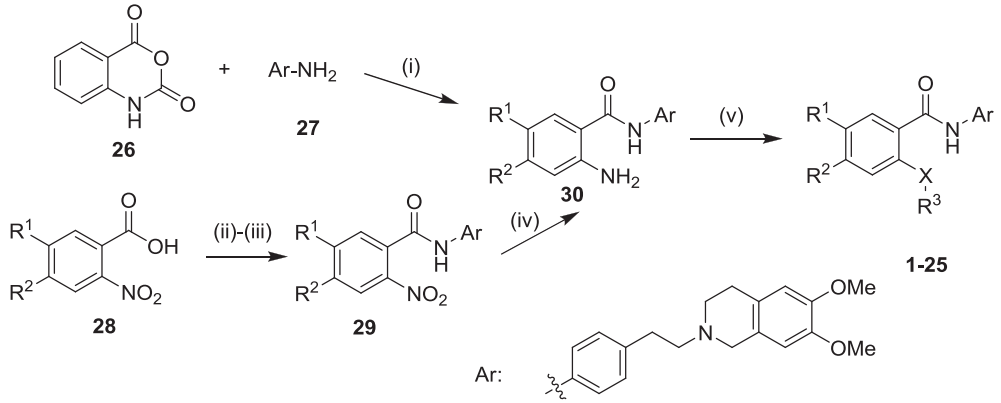

Scheme 1. Preparation of *N*-(4-(2-(6,7-dimethoxy-3,4-dihydroisoquinolin-2(1*H*)-yl)ethyl)phenyl)-2-(substituted phenylsulfonamido)benzamides. Reagents and conditions: (i) CH_3CN, CH_3COOH (85%); (ii) $SOCl_2$, 83 °C, reflux, 2 h; (iii) Ar–NH_2 (**27**), $NaHCO_3$, CH_2Cl_2, 0 °C to r.t., 5 h (80%); (iv) Pd/C, H_2/$HCOONH_4$, CH_3OH, reflux, 4–6 h (85%); (v) R^3SO_2Cl, pyridine, CH_2Cl_2, r.t. or R^3COCl, $NaHCO_3$, CH_2Cl_2, r.t. (75–95%).

Table 1
Structures of the compounds studied.

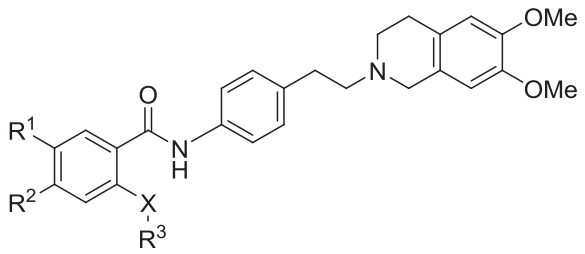

Code	R^1	R^2	X	R^3
1	H	H	N	*bis*-Phenylsulfonyl
2	H	H	$NHSO_2$	2,4,6-Trimethylphenyl
3	H	H	$NHSO_2$	4-(Trifluoromethyl)phenyl
4	H	H	$NHSO_2$	4-Acetamidophenyl
5	H	H	N	*bis*-(4-bromophenylsulfonyl)
6	H	H	$NHSO_2$	5-(Dimethylamino)naphthalene-
7	H	H	$NHSO_2$	2-Propyl
8	H	H	$NHSO_2$	2-(Trifluoromethyl)phenyl
9	H	H	$NHSO_2$	2-Fluorophenyl
10	H	H	$NHSO_2$	4-Chlorophenyl
11	H	H	$NHSO_2$	4-*tert*-Butylphenyl
12	H	H	$NHSO_2$	4-Fluorophenyl
13	H	H	$NHSO_2$	2,5-Dichlorophenyl
14	H	H	$NHSO_2$	4-Methylphenyl
15	H	H	$NHSO_2$	4-Methoxyphenyl
16	OMe	OMe	$NHSO_2$	4-*tert*-Butylphenyl
17	OMe	OMe	$NHSO_2$	4-(Trifluoromethyl)phenyl
18	OMe	OMe	$NHSO_2$	4-Methylphenyl
19	H	H	HN–C(=O)–O	(9H-Fluoren-9-yl)methyl
20	H	H	NHCO	Undecane-
21	H	H	NHCO	(*E*)-Cinnamyl
22	H	H	NHCO	4-Fluoro-2-nitrobenzyl
23	H	H	NHCO	2-Furanyl
24	H	H	NHCO	3-Quinolinyl
25	OMe	OMe	NHCO	3-Quinolinyl

Using tariquidar as the positive control (set as 100% UIC2 labeling for comparison), the tariquidar derivatives interacting with P-gp identified from the efflux assay (**24**, **16**, **5**, **21**, **23** & **22**) were found to notably increase UIC2 labeling. UIC2 shift caused by these tariquidar derivatives were found to be 93.2 ± 7.2%, 70.7 ± 2.8%, 47.0 ± 1.0%, 46.3 ± 0.9%, 35.5 ± 2.7% and 57.3 ± 2.5%, respectively, relative to the level attained by tariquidar. As negative controls, the ineffective P-gp tariquidar derivatives (**11** and **14**; chosen to represent the two different chemical series) did not give rise to detectable UIC2 shift (Fig. 4A). Similarly, the tariquidar derivatives interacting with BCRP (**24**, **21**, **23** and **22**) were all found to generate remarkable 5D3 shift as to 90.7 ± 2.1%, 118.6 ± 7.4%, 149.4 ± 5.8% and 119.1 ± 6.3%, respectively, relative to the level attained by the parent tariquidar, suggesting their interaction with the BCRP transporter. As negative controls, the ineffective BCRP tariquidar derivatives (**11** and **14**; chosen to represent the two different chemical series) did not result in any appreciable 5D3 shift (Fig. 4B). Of note, consistent with the dual specificity of **24** in inhibiting P-gp and BCRP, this tariquidar derivative was found to result in both remarkable UIC2 and 5D3 shift.

2.2.5. Effect of tariquidar derivatives on the ATPase activity of P-gp and BCRP

Drug transport activity of P-gp and BCRP are associated with ATP hydrolysis that may be modulated by substrates or inhibitors of the transporters. To further understand the mechanism of P-gp and BCRP inhibition by the tariquidar derivatives, vanadate-sensitive ATPase activity of both transporters was measured in the presence of a range of different concentrations of the tested compounds. Similar to tariquidar, **24**, **16**, **5**, **21**, **23** and **22** were found to inhibit P-gp ATPase activity in a concentration-dependent manner (Fig. 5A). The relative rank of maximum P-gp ATPase inhibition by these tested tariquidar derivatives were found to be consistent with their inhibitory effect on P-gp efflux activity. On the other hand, tariquidar was found to stimulate BCRP ATPase activity, which agreed well with literature-reported observation [27]. Similarly, the BCRP-inhibiting tariquidar derivatives (**24**, **22**, **21** and **23**) were all found to stimulate BCRP ATPase (Fig. 5B), the extent of which parallel their BCRP inhibitory activity. Therefore, mechanistically, similar to tariquidar, the new derivatives are likely competitive inhibitor to BCRP. They behave like BCRP substrates and stimulate ATP hydrolysis. On the other hand, both tariquidar and the new derivatives inhibit P-gp transport function by inhibiting the ATPase activity (i.e. energy source) of the transporter.

3. Conclusions

A series of tariquidar analogs were synthesized and evaluated for P-gp and BCRP inhibitory activity. Synthetic methods of anthranilic sulfonamides reported in this study allowed the preparation of a diverse array of sulfonated derivatives of anthranilamides. The synthesized compounds, especially those sulfonamide compounds (**1**, **5**, **10**, **13**, **16** and **17**), exhibited low toxicity and better aqueous solubility than the lead compound tariquidar. Among the tariquidar derivatives evaluated, **21**, **22**, **23**, **24** (from the amide series) were found to dually inhibit P-gp and BCRP-mediated drug efflux. The structural modification in **1**, **5** and **16** (the sulfonamide series) made them specific towards P-gp. When the 3-quinoline carboxylic amide moiety (BB3) was replaced with sulfonamide, the P-gp inhibitory activity retained, suggesting that the 3-quinoline structure was not an essential group for their activity. Without influencing cell proliferation, the new tariquidar derivatives were found to potentiate the cytotoxicity of the anticancer drugs which were the transporter substrate anticancer drug in the corresponding transporter-overexpressing cell line.

Table 2
Effect of the compounds on cell viability of cancer cells and normal epithelial cells.

Compounds	Cancer cell lines (48 h)			Normal colon cell (48 h)	Normal gastric cell (72 h)
	HCT116 IC_{50} (μM)	SW620 IC_{50} (μM)	SW620-Ad300 IC_{50} (μM)	CCD18-Co IC_{50} (μM)	HFE IC_{50} (μM)
Tariquidar	12.5 ± 0.8	25 ± 1.9	25 ± 2.1	25 ± 1.7	1.28 ± 0.06
3, **13**, **17**	25	>100	>100	>100	>100
1, **5**, **10**, **16**, **24**	>100	>100	>100	>100	>5
21	>100	>100	>100	>100	>20
22	>100	>100	>100	>100	>10
Other derivatives	>100	>100	>100	>100	>100

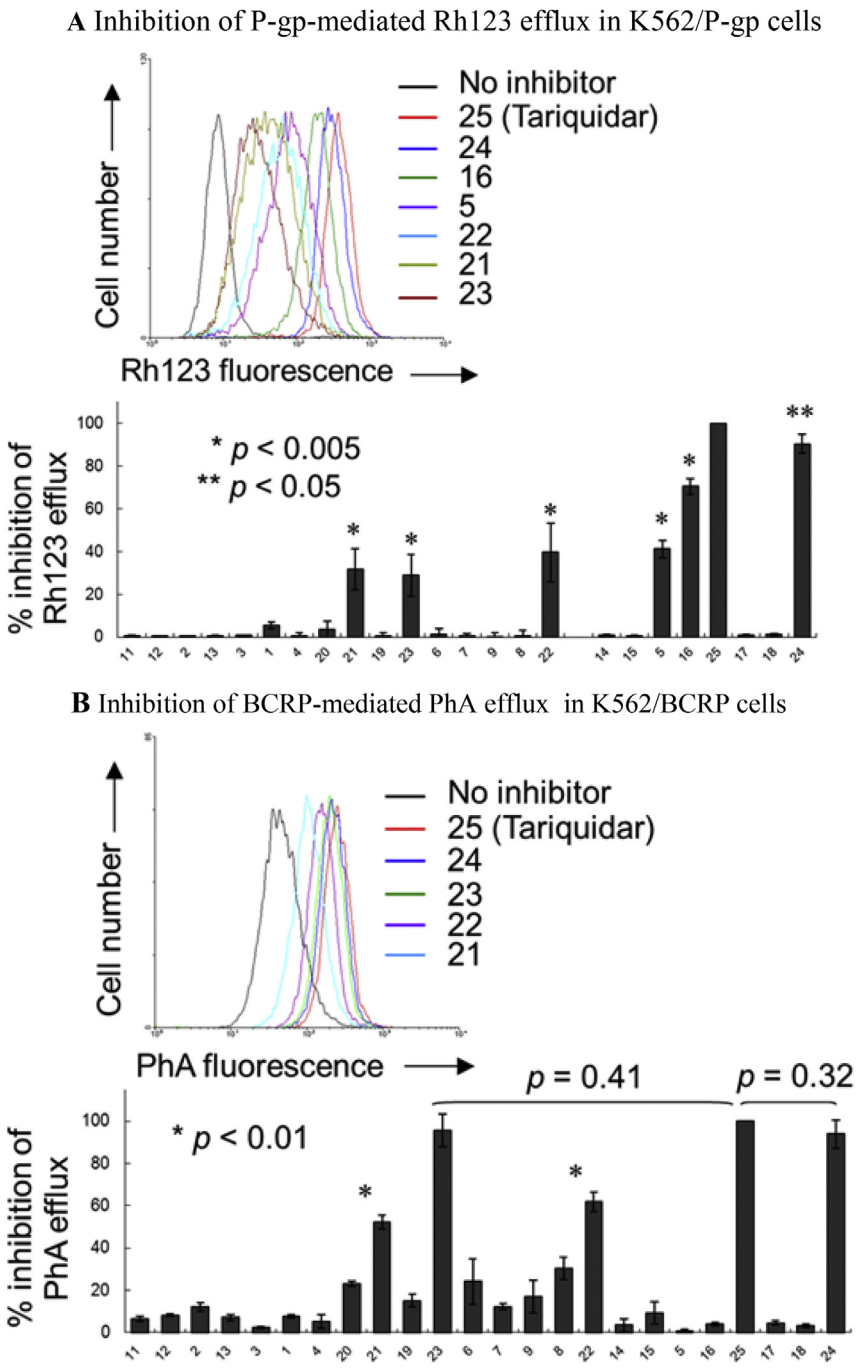

Fig. 3. Inhibition of P-gp-mediated Rh123 efflux (A) and BCRP-mediated PhA efflux (B) in K562/P-gp and K562/BCRP cells, respectively. (A) K562/P-gp cells were incubated with 0.5 μg/mL Rh123 alone (black), 0.5 μg/mL Rh123 and 0.5 μM tariquidar (25) (red), or 0.5 μg/mL Rh123 and 0.5 μM of the various tariquidar derivatives (other colors) at 37 °C for 30 min. Retention of Rh123 fluorescence in cells after 1h of Rh123-free efflux was measured by flow cytometry. Representative histogram for the inhibition of Rh123 efflux from three independent experiments was shown in the upper panel. The results were presented as % inhibition of Rh123 efflux relative to the parent tariquidar in the lower panel. Columns, means of triplicate determinations; bars, SD. $^{*}p < 0.01$ versus tariquidar (statistically analysis is only shown for the P-gp-inhibiting derivatives. (B) Cells were incubated with 1 μM of PhA alone (black), 1 μM of PhA and 0.5 μM of tariquidar (25) (red), or 1 μM of PhA and 0.5 μM of various tariquidar derivatives at 37 °C for 30 min. PhA fluorescence retention in the cells after 1 h of PhA-free efflux was measured by flow cytometry. Representative histogram for the inhibition of PhA efflux from three independent experiments was shown in the upper panel. The results were also presented as % inhibition of PhA efflux relative to tariquidar in the lower panel. Columns means of triplicate determinations; bars means SD. $^{*}p < 0.01$ vs tariquidar. (For interpretation of the references to color in this figure legend, the reader is referred to the web version of this article.)

Importantly, the extent of resistance reversal was found to be consistent with the transporter inhibitory activity of the new derivatives. Increased UIC2 or 5D3 labeling by effective tariquidar derivatives (**24**, **16**, **5**, **21**, **23** and **22**) further suggested their interaction with P-gp and BCRP. In addition, we also showed that P-gp and BCRP inhibition by the tariquidar derivatives was associated with the inhibition of ATP hydrolysis. In summary, our study identified promising and safe inhibitors of MDR transporters with higher inhibitory effect than verapamil (2nd generation P-gp inhibitor) and comparable effect as tariquidar (the most potent and selective P-gp inhibitor reported to date). Further development of **1**, **5** are warranted to appreciate more fully their potential in MDR circumvention.

Table 3
Reversal of multidrug resistance by new tariquidar derivatives.

	IC_{50} ± SD (fold resistance)[a]	
	LCC6	LCC6 MDR (P-gp)
Paclitaxel	1.06 ± 0.15 nM (1)	132.3 ± 15.4 nM (125)
+200 nM Tariquidar	1.32 ± 0.19 nM (1.1)	2.45 ± 0.33 nM (1.9)**
+200 nM compound **5**	1.44 ± 0.32 nM (1.3)	52.4 ± 6.9 nM (36)*
+200 nM compound **16**	1.29 ± 0.26 nM (1.0)	26.5 ± 5.2 nM (21)*
+200 nM compound **24**	1.09 ± 0.37 nM (0.9)	3.02 ± 0.41 nM (2.8)**
+200 nM compound **21**	1.72 ± 0.21 nM (1.6)	56.8 ± 7.1 nM (33)*
+200 nM compound **23**	1.35 ± 0.26 nM (1.3)	62.5 ± 7.6 nM (46)*
+200 nM compound **22**	1.12 ± 0.16 nM (1.1)	39.5 ± 4.2 nM (35)*
	MCF-7	MCF-7 FLV1000 (BCRP)
Mitoxantrone	11.3 ± 4.2 nM (1)	2350 ± 380 nM (208)
+200 nM Tariquidar	9.5 ± 3.2 nM (0.8)	35 ± 26 nM (3.7)**
+200 nM compound **24**	14.5 ± 5.1 nM (1.3)	42 ± 22 nM (2.9)**
+200 nM compound **21**	17.5 ± 6.2 nM (1.5)	1120 ± 420 nM (64)*
+200 nM compound **23**	15.5 ± 6.8 nM (1.4)	32 ± 25 nM (2.1)**
+200 nM compound **22**	18.8 ± 4.9 nM (1.7)	860 ± 440 nM (46)*
	IC_{50} ± SD (fold resistance) HepG2	R-HepG2 (P-gp)
Doxorubicin	7.486 ± 0.112 μM (1)	97.19 ± 2.1 μM (12.98)
+200 nM Tariquidar	1.723 ± 0.019 μM (0.23)	2.4 ± 0.13 μM (0.32)**
+200 nM compound **22**	5.657 ± 0.035 μM (0.76)	2.71 ± 0.09 μM (0.36)**
+200 nM compound **23**	8.13 ± 0.014 μM (1.09)	22.45 ± 1.501 μM (3.00)*
+200 nM compound **24**	2.158 ± 0.033 μM (0.29)	2.858 ± 0.13 μM (0.38)**
	SW620	SW620-AD300 (p-gp)
Doxorubicin	92.89 ± 21.2 nM (1)	1360 ± 138.2 nM (14.64)
+200 nM Tariquidar	53.33 ± 12.3 nM (0.57)	172 ± 21.6 nM (1.85)***
+200 nM compound **22**	149 ± 15.1 nM (1.6)	336.3 ± 20.1 nM (3.62)***
+200 nM compound **23**	194.8 ± 26.2 nM (2.1)	243.9 ± 14.2 nM (2.63)***
+200 nM compound **24**	33.88 ± 9.8 nM (0.36)	579.1 ± 23.3 nM (6.23)***

*$p < 0.05$; compared with the anticancer drug alone in the resistant cell line.
**$p < 0.01$; compared with the anticancer drug alone in the resistant cell line.
***$p < 0.001$; compared with the anticancer drug alone in the resistant cell line.
[a] Fold resistance of the anticancer drug tested was indicated in parenthesis. It is defined as the IC_{50} of the anticancer drug in the resistant cells/that in the parental cells.

4. Experimental section

4.1. Chemistry

4.1.1. Materials and methods

Chemicals and reagents were purchased from commercial suppliers and used without special instructions. Products were detected by TLC on alumina plates coated with silica gel (Merck silica gel 60 F254, thickness 0.2 mm) and visualized by UV light (λ 254 nm). Column chromatographic separations were performed by using silica gel (Merck silica gel Si 60, particle size 40–63 μm, 230–300 mesh). Melting points were determined with a Yanako MP-500D and are uncorrected. Mass spectra were recorded with Finnigan MAT TSQ 7000 (ESI). IR spectra recorded with a SHIMADZU FTIR-8400S spectrometer. NMR spectra were recorded with Bruker Avance 400 (^{1}H: 400.1 MHz; ^{13}C: 100.6 MHz; *T*: 300 K) instrument. The used solvent for each spectrum is reported. The chemical shift values are expressed in parts per million (ppm) relative to the internal standard tetramethylsilane and coupling constants *J* are given in Hz. Abbreviations are as follows: s, singlet; d, doublet; t, triplet; m, multiplet; br, broad; dd, double doublet. The relative numbers of protons is determined by integration. Purification was performed using silica gel column chromatography, unless otherwise noted.

4.1.2. General procedure for the synthesis of compounds ***1***–***25***

The general synthetic route for the title compounds comprises the formation of aromatic amine (**30**) and subsequent sulfonamide or amide bond. Isatoic anhydride can react with the amine **27**, which directly gave **30**. Another method was the formation of an amide bond between 2-nitrobenzoic acid and the aromatic amine **27**, which was synthesized as described before. Subsequent reduction of the nitro group to give aromatic amines **30**, afterward, **30** were reacted with sulfonyl chloride in dichloromethane catalyzed by pyridine to generate **1**–**18** in good yields. Acylation of the resulting 2-aminobenzamides **30** with the appropriate carboxylic acid chloride R′COCl yielded the compounds **19**–**25**.

4.1.3. General procedure A for the preparation of carbonyl chlorides

The corresponding carboxylic acid was suspended in $SOCl_2$ (10–15 mL), then DMF was added dropwisely as catalyst, the mixture was heated at 83 °C for 2 h. Excess $SOCl_2$ was removed under reduced pressure, and the resulting solid was dried under vacuum.

4.1.4. General procedures B and C for the preparation of the aromatic amine (***30***)

(B) Starting from isatoic anhydride: To a solution of acetonitrile (25 mL) containing 1.56 g of 4-[2-(3,4-dihydro-6,7-dimethoxy-2(1*H*)-isoquinolinyl)ethyl]benzenamine (5 mmol, 1 eq.) was added 0.89 g of isatoic anhydride (5.5 mmol, 1.1 eq.), and the mixture was stirred under reflux for 10 h, after adding 0.5 mL acetic acid, the mixture was refluxed for another 10 h, and the solvents were removed under vacuum, the deposit was dissolved in CH_2Cl_2, washed with saturated aqueous solution of $NaHCO_3$ (3×), dried over $MgSO_4$, and concentrated to give the crude product, which was

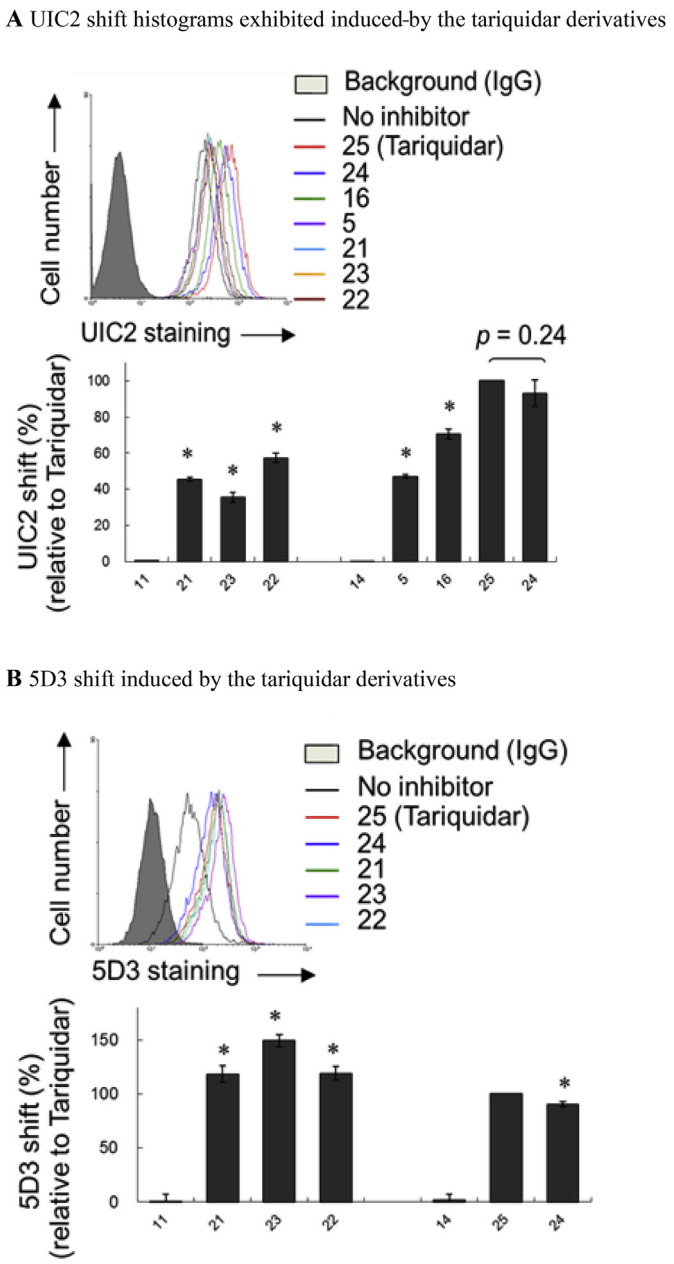

Fig. 4. UIC2/5D3 labeling in intact P-gp/BCRP-overexpressing K562 cells suggesting the interaction between the effective tariquidar derivatives and the two transporters. (A) UIC2 shift histograms generated by the tariquidar derivatives (upper panel). The solid black line represents UIC2 labeling of the untreated (native) cells, red line for the cells incubated with 0.5 μM tariquidar, or lines with various colors for cells incubated with 0.5 μM of the tariquidar derivatives. The shaded histogram represents the background fluorescent signal upon labeling with a mouse IgG2b (isotype control). The results were presented as % UIC2 shift relative to the parent tariquidar (set as 100%) in the lower panel. $^{*}p < 0.005$, versus tariquidar (statistical analysis is only shown for the P-gp-inhibiting derivatives. **11** and **14** were also tested as the negative control (non-P-gp-inhibiting derivatives) to represent the two different chemical series. (B) 5D3 shift produced by the tariquidar derivatives (upper panel). Similar color codes are adopted as with UIC2 labeling in (A) above. The results were presented as % 5D3 shift relative to the parent tariquidar (set as 100%) in the lower panel. $^{*}p < 0.05$, versus tariquidar (statistical analysis is only shown for the BCRP-inhibiting derivatives. **11** and **14** were also tested as the negative control (non-BCRP-inhibiting derivatives) to represent the two different chemical series. (For interpretation of the references to color in this figure legend, the reader is referred to the web version of this article.)

purified by column chromatography on silica gel yielding 85% of **30** through one step.

(C) Starting from o-nitrobenzoylic acid: o-Nitrobenzoylic acid

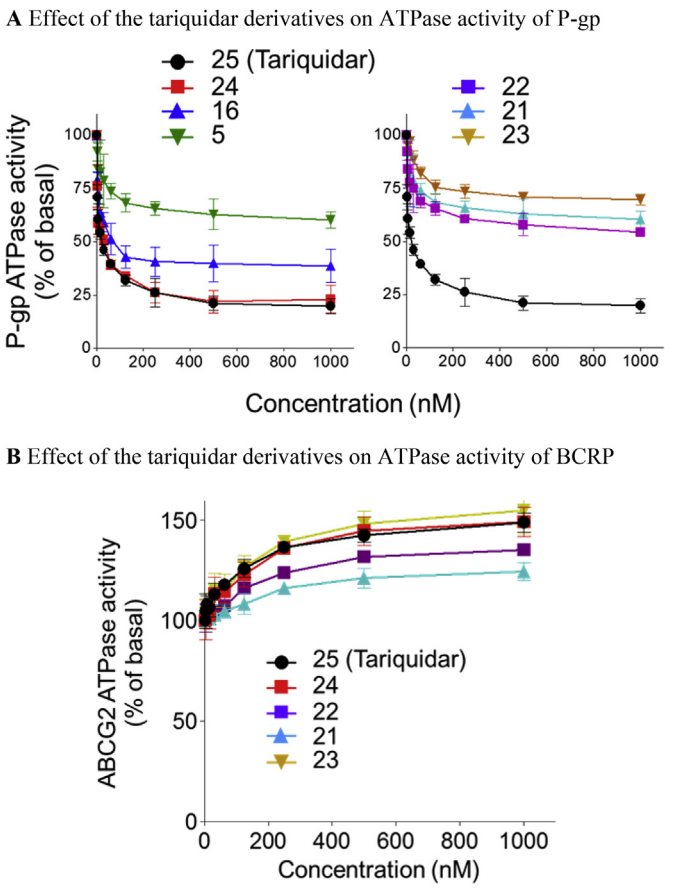

Fig. 5. Effect of the tariquidar derivatives on ATPase activity of P-gp (A) and BCRP (B). Vanadate-sensitive P-gp and BCRP ATPase activity was determined as described in the Experimental section. Only the tariquidar derivatives with P-gp- or BCRP-inhibitory activity were evaluated. The average % difference in activity from the basal ATPase activity in two independent experiments with three individual measurements was presented. The error bars represent standard deviation.

(or 6-Nitroveratric acid) chloride was obtained via procedure A. Acylation of 4-(2-(6,7-dimethoxy-3,4-dihydroisoquinolin-2(1*H*)-yl)ethyl)aniline (**27**) with an o-nitrobenzoyl chloride in dichloromethane using sodium hydrogen carbonate as base. The corresponding nitro compound **29** (3.3 mmol, 1 eq.) was dissolved in methanol, palladium on activated charcoal (10% m/m) and 1.66 g of $HCOONH_4$ (26.4 mmol, 8 eq.) were added, and the solution was stirred under reflux for 4 h. Then, the catalyst and unreacted $HCOONH_4$ were filtered off, and the solvents were removed under vacuum. The deposit was dissolved in H_2O and extracted with CH_2Cl_2 (3×), concentrated to give the crude product, which was purified by column chromatography on silica gel yielding 68% of **30**.

*4.1.5. General procedures D for the preparation of the sulfonamide bonds **1**–**18***

The aromatic amine (**30**) (1 eq.) and pyridine (3 eq.) were dissolved in CH_2Cl_2, and the benzene sulfonyl chloride was added in small portions. The solution was stirred at room temperature for 2–4 h, the solution was diluted with CH_2Cl_2, washed with water (2×) and saturated aqueous solution of $NaHCO_3$ (3×), dried over $MgSO_4$, and concentrated to give the crude product, which was purified by column chromatography using silica gel. Synthesis of sulfonamide anthranilamides analog was carried out in analogy to the synthesis of derivatives.

4.1.6. General procedures E for the preparation of the amide bonds **19–24**

The aromatic amine (**30**) (1 eq.) and NEt_3 (3 eq.) were dissolved in CH_2Cl_2, and the aromatic carbonyl chloride (1.5 eq.) derived from the corresponding acid via general procedure A was added in small portions. The solution was stirred at room temperature for 24 h, diluted with CH_2Cl_2, washed with water and saturated aqueous solution of Na_2CO_3 (3×), dried over $MgSO_4$, and concentrated to give the crude product, which was purified by column chromatography using silica gel or recrystallization.

4.1.7. N-(4-(2-(6,7-Dimethoxy-3,4-dihydroisoquinolin-2(1H)-yl) ethyl)phenyl)-2-(N-(phenylsulfonyl)phenylsulfonamido)benzamide (**1**)

The compound was synthesized following general procedure C and D, purified by column chromatography on silica gel (8.3% MeOH/CH_2Cl_2, $R_f = 0.3$). The product was obtained as a pale-yellow powder (79% yield), mp: 196–198 °C. ^{1}HNMR (400 MHz, $CDCl_3$): δ(ppm) = 2.74–2.87 (m, 8H, $-CH_2-$), 3.65 (s, 2H, $-N-CH_2-Ar$), 3.83 (s, 6H, Ar$-OCH_3$), 6.54 (s, 1H, Ar–H), 6.59 (s, 1H, Ar–H), 7.08 (d, 2H, $J = 8.4$ Hz, Ar–H), 7.31 (d, 2H, $J = 8.4$ Hz, Ar–H), 7.350–7.380 (m, 1H, Ar–H), 7.40 (d, 4H, $J = 8.4$ Hz, Ar–H), 7.51 (d, 2H, $J = 7.6$ Hz, Ar–H), 7.55 (d, 2H, $J = 8.8$ Hz, Ar–H), 7.78 (q, 1H, $^3J = 8.0$ Hz, $^4J = 1.4$ Hz, Ar–H), 7.96 (d, 4H, $J = 7.6$ Hz, Ar–H), 9.14 (s, 1H, Ar–CONH–Ar). IR ν_{max} (KBr): 3444.63, 2921.96, 2850.59, 2389.64, 2302.85, 1676.03, 1650.95, 1604.66, 1515.94, 1452.3, 1375.15, 1257.5, 1166.85, 1124.42, 1083.92, 1016.42, 910.34, 862.12, 756.04 cm^{-1}. ESI-MS (m/z): 711.097 $[M]^+$.

4.1.8. N-(4-(2-(6,7-Dimethoxy-3,4-dihydroisoquinolin-2(1H)-yl) ethyl)phenyl)-2-(2,4,6-trimethylphenylsulfonamido)benzamide (**2**)

The compound was synthesized following general procedure C and D, purified by column chromatography on silica gel (12.5% MeOH/CH_2Cl_2, $R_f = 0.34$) to obtain a pale-yellow solid (90% yield), mp: 123–124 °C. ^{1}HNMR (400 MHz, $CDCl_3$): δ(ppm) = 2.21 (s, 3H, Ar$-CH_3$), 2.62 (s, 6H, Ar$-CH_3$), 2.82–3.08 (m, 8H, $-CH_2-$), 3.81 (s, 2H, –CONH–Ar), 3.86 (s, 3H, Ar$-OCH_3$), 3.87 (s, 3H, Ar$-OCH_3$), 5.32 (s, 1H, $-SO_2NH-$), 6.55 (s, 1H, Ar–H), 6.62 (s, 1H, Ar–H), 6.85 (s, 2H, Ar–H), 7.05 (m, 1H, Ar–H), 7.242 (d, 2H, $J = 8.4$ Hz, Ar–H), 7.36 (d, 2H, $J = 7.6$ Hz, Ar–H), 7.49 (d, 2H, $J = 8.4$ Hz, Ar–H), 7.58 (d, 1H, $J = 7.6$ Hz, Ar–H), 7.97 (s, 1H, –CONH–). IR ν_{max} (KBr): 3444.63, 2931.60, 2839.02, 1643.24, 1600.81, 1515.94, 1456.16, 1377.08, 1328.86, 1257.50, 1228.57, 1155.28, 1118.64, 1053.06, 827.41, 754.12 cm^{-1}. ESI-MS (m/z): 612.947 $[M-1]^+$.

4.1.9. N-(4-(2-(6,7-Dimethoxy-3,4-dihydroisoquinolin-2(1H)-yl) ethyl)phenyl)-2-(4-(trifluoromethyl)phenylsulfonamido)benzamide (**3**)

The compound was synthesized following general procedure C and D, purified by column chromatography on silica gel (10% MeOH/CH_2Cl_2, $R_f = 0.4$), The product was obtained as a white colored crystal (81% yield), mp: 137–139 °C. ^{1}HNMR (400 MHz, $CDCl_3$): δ(ppm) = 2.78–2.95 (m, 8H, $-CH_2-$), 3.69 (s, 2H, $-N-CH_2-Ar$), 3.833 (s, 3H, Ar$-OCH_3$), 3.842 (s, 3H, Ar$-OCH_3$), 6.53 (s, 1H, Ar–H), 6.60 (s, 1H, Ar–H), 7.14 (t, 1H, $J = 7.4$ Hz, Ar–H), 7.247 (t, 2H, $J = 7.8$ Hz, Ar–H), 7.38 (d, 2H, $J = 8.0$ Hz, Ar–H), 7.44 (t, 1H, $J = 7.8$ Hz, Ar–H), 7.54 (d, 1H, $J = 8.4$ Hz, Ar–H), 7.57 (d, 2H, $J = 8.0$ Hz, Ar–H), 7.64 (d, 1H, $J = 8.0$ Hz, Ar–H), 7.88 (d, 2H, $J = 8.0$ Hz, Ar–H). IR ν_{max} (KBr): 3448.49, 3010.67, 2931.6, 1643.24, 1602.74, 1542.95, 1517.87, 1465.8, 1400.22, 1325.01, 1261.36, 1236.29, 1168.78, 1126.35, 1089.71, 983.63, 837.05, 756.04 cm^{-1}. ESI-MS (m/z): 639.20 $[M]^+$.

4.1.10. 2-(4-Acetamidophenylsulfonamido)-N-(4-(2-(6,7-dimethoxy-3,4-dihydroisoquinolin-2(1H)-yl)ethyl)phenyl) benzamide (**4**)

The compound was synthesized following general procedure C and D, purified by column chromatography on silica gel (8.3% MeOH/CH_2Cl_2, $R_f = 0.35$), The product was obtained as a pale yellow needle crystal (87% yield), mp: 200–202 °C. ^{1}HNMR (400 MHz, $CDCl_3$): δ(ppm) = 2.09 (s, 3H, $-COCH_3$), 2.81–2.92 (m, 8H, $-CH_2-$), 3.73 (s, 2H, $-N-CH_2-Ar$), 3.777 (s, 3H, Ar$-OCH_3$), 3.779 (s, 3H, Ar$-OCH_3$), 6.664 (s, 1H, Ar–H), 6.70 (s, 1H, Ar–H), 7.02 (t, 1H, $J = 6.6$ Hz, Ar–H), 7.20 (d, 2H, $J = 7.6$ Hz, Ar–H), 7.33 (t, 1H, $J = 7.8$ Hz, Ar–H), 7.47 (d, 1H, $J = 8.4$ Hz, Ar–H), 7.52 (q, 4H, $^3J = 8.8$ Hz, $^4J = 2.4$ Hz), 7.62 (d, 2H, $J = 8.8$ Hz, Ar–H), 7.8 (d, 1H, $J = 7.6$ Hz, Ar–H). IR ν_{max} (KBr): 3743.57, 3450.41, 3101.32, 3035.75, 2929.67, 2356.85, 1693.38, 1643.24, 1595.02, 1519.8, 1461.94, 1404.08, 1371.29, 1325.01, 1259.43, 1157.21, 1122.49, 1087.78, 838.98 cm^{-1}. ESI-MS (m/z): 627.088 $[M-1]^+$.

4.1.11. 2-(4-Bromo-N-(4-bromophenylsulfonyl) phenylsulfonamido)-N-(4-(2-(6,7-dimethoxy-3,4-dihydroisoquinolin-2(1H)-yl)ethyl)phenyl)benzamide (**5**)

The compound was synthesized following general procedure C and D, purified by column chromatography on silica gel (8.3% MeOH/CH_2Cl_2, $R_f = 0.443$), The product was obtained as a light yellow powder (82% yield), mp: 165–167 °C. ^{1}HNMR (400 MHz, $CDCl_3$): δ(ppm) = 2.75–2.93 (m, 8H, $-CH_2-$), 3.70 (s, 2H, $-N-CH_2-Ar$), 3.831 (s, 3H, Ar$-OCH_3$), 3.834 (s, 3H, Ar$-OCH_3$), 6.54 (s, 1H, Ar–H), 6.59 (s, 1H, Ar–H), 6.69 (d, 1H, $J = 8.0$ Hz, Ar–H), 7.13 (d, 2H, $J = 8.4$ Hz, Ar–H), 7.29 (d, 2H, $J = 8.4$ Hz, Ar–H), 7.40 (t, 1H, $J = 7.6$ Hz, Ar–H), 7.51 (d, 4H, $J = 8.8$ Hz, Ar–H), 7.58 (t, 1H, $J = 7.6$ Hz, Ar–H), 7.81 (d, 1H, $J = 7.6$ Hz, Ar–H), 7.80 (d, 4H, $J = 8.4$ Hz, Ar–H), 9.00 (s, 1H, Ar–CONH–Ar). IR ν_{max} (KBr): 3741.65, 3672.21, 2927.74, 2312.49, 1677.95, 1515.94, 1384.79, 1166.85, 1008.7, 910.34, 862.12, 821.62 cm^{-1}. ESI-MS (m/z): 869.941 $[M-1]^+$.

4.1.12. N-(4-(2-(6,7-Dimethoxy-3,4-dihydroisoquinolin-2(1H)-yl) ethyl)phenyl)-2-(5-(dimethylamino)naphthalene-1-sulfonamido) benzamide (**6**)

The compound was synthesized following general procedure B and D, purified by column chromatography on silica gel (6.7% MeOH/CH_2Cl_2, R_f = 0.42). The product was obtained as a light yellow powder (76% yield), mp: 176–178 °C. ^{1}HNMR (400 MHz, DMSO-d_6): δ(ppm) = 2.74–2.78 (m, 8H, $-CH_2-$), 3.06 (s, 6H, $-N-CH_3$), 3.70 (s, 6H, Ar$-OCH_3$), 3.75 (s, 2H, $-N-CH_2-Ar$), 6.59–6.77 (m, 4H, Ar–H), 7.03 (d, 2H, $J = 8.0$ Hz, Ar–H), 7.21 (d, 3H, $J = 4.0$ Hz, Ar–H), 7.26 (d, 1H, $J = 7.2$ Hz, Ar–H), 7.55 (s, 4H, Ar–H), 7.88 (d, 1H, $J = 6.8$ Hz, Ar–H), 8.17 (d, 1H, $J = 4.0$ Hz, Ar–H), 8.26 (d, 1H, $J = 8.0$ Hz, Ar–H), 8.66 (d, 1H, $J = 8.0$ Hz, Ar–H), 14.1 (s, 1H, –NH–). IR ν_{max} (KBr): 3450.41, 2933.53, 2831.31, 2783.09, 1637.45, 1604.66, 1432.18, 1352.23, 1336.07, 1137.26, 1056.31, 857.58 cm^{-1}. ESI-MS (m/z): 663.28 $[M-1]^+$.

4.1.13. N-(4-(2-(6,7-Dimethoxy-3,4-dihydroisoquinolin-2(1H)-yl) ethyl)phenyl)-2-(propylsulfonamido)benzamide (**7**)

The compound was synthesized following general procedure B and D, purified by column chromatography on silica gel (6.7% MeOH/CH_2Cl_2, $R_f = 0.2$). The product was obtained as a light yellow powder (93% yield), mp: 137–139 °C. ^{1}HNMR (400 MHz, DMSO-d_6): δ(ppm) = 0.9 (s, 3H, $-CH_2-CH_3-$), 1.63–1.65 (m, 2H, $-CH_2-CH_3$), 2.72–2.80 (m, 8H, $-CH_2-$), 3.00 (s, 2H, $-CH_2-SO_2-$), 3.60 (s, 2H, $-N-CH_2-Ar$), 3.69 (s, 6H, Ar$-OCH_3$), 6.64 (s, 1H, Ar–H), 6.65 (s, 1H, Ar–H), 6.93 (s, 1H, Ar–H), 7.21 (d, 2H, $J = 8.0$ Hz, Ar–H), 7.35 (s, 1H, Ar–H), 7.48 (d, 1H, $J = 8.0$ Hz, Ar–H), 7.60 (d, 2H, $J = 8.0$ Hz, Ar–H), 7.92 (d, 1H, $J = 8.0$ Hz, Ar–H), 10.3 (s, 1H, –CO–NH–). IR ν_{max} (KBr):

3735.86, 3624, 2933.53, 2827.45, 2352.99, 1639.38, 1604.66, 1413.08, 1346.29, 1315.62, 1253.74, 1165.28, 1065.44, 838.98 cm^{-1}. ESI-MS (*m*/*z*): 536.419 $[M-1]^+$.

4.1.14. N-(4-(2-(6,7-Dimethoxy-3,4-dihydroisoquinolin-2(1H)-yl) ethyl)phenyl)-2-(2-(trifluoromethyl)phenylsulfonamido)benzamide (**8**)

The compound was synthesized following general procedure B and D, purified by column chromatography on silica gel (10% MeOH/CH_2Cl_2, $R_f = 0.4$). The product was obtained as a light yellow powder (84% yield), mp: 152–154 °C. ^{1}HNMR (400 MHz, DMSO-d_6): δ(ppm) = 2.94–3.24 (m, 8H, $-CH_2-$), 3.71 (s, 3H, Ar–OCH_3), 3.72 (s, 3H, Ar–OCH_3), 4.20 (s, 2H, $-N-CH_2-Ar-$), 6.66 (s, 1H, Ar–H), 6.75 (s, 1H, Ar–H), 6.77 (s, 1H, Ar–H), 7.07 (s, 1H, Ar–H), 7.24 (d, 2H, *J* = 8.0 Hz, Ar–H), 7.65 (d, 2H, *J* = 7.6 Hz, Ar–H), 7.62 (t, 1H, *J* = 8.0 Hz, Ar–H), 7.71 (t, 1H, *J* = 7.6 Hz, Ar–H), 7.79 (d, 1H, *J* = 7.6 Hz, Ar–H), 7.97 (d, 1H, *J* = 7.6 Hz, Ar–H), 8.20 (d, 1H, *J* = 7.6 Hz, Ar–H), 9.90 (s, 1H, –NH–). IR ν_{max} (KBr): 3739.72, 3510.2, 3448.49, 3004.89, 2839.02, 2592.15, 2358.78, 1836.11, 1743.53, 1641.31, 1521.73, 1460.01, 1313.43, 1257.5, 1128.28, 977.84, 908.41, 838.98, 767.62 cm^{-1}. ESI-MS (*m*/*z*): 638.123 $[M-1]^+$.

4.1.15. N-(4-(2-(6,7-Dimethoxy-3,4-dihydroisoquinolin-2(1H)-yl) ethyl)phenyl)-2-(2-fluorophenylsulfonamido)benzamide (**9**)

The compound was synthesized following general procedure B and D, purified by column chromatography on silica gel (10% MeOH/EA, $R_f = 0.25$). The product was obtained as a light yellow powder (82% yield), mp: 203–205 °C. ^{1}HNMR (400 MHz, DMSO-d_6): δ(ppm) = 2.95–3.0 (m, 3H, $-CH_2-$), 6.76 (s, 1H, Ar–H), 6.79 (s, 1H, Ar–H), 7.17 (d, 1H, *J* = 8.8 Hz, Ar–H), 7.21 (d, 1H, *J* = 3.6 Hz, Ar–H), 7.26 (d, 2H, *J* = 8.4 Hz, Ar–H), 7.31 (d, 1H, *J* = 8.4 Hz, Ar–H), 7.48–7.49 (m, 1H, Ar–H), 7.67 (d, 2H, *J* = 8.4 Hz, Ar–H), 7.82–7.86 (m, 1H, Ar–H), 7.91 (d, 1H, *J* = 8.0 Hz, Ar–H). IR ν_{max} (KBr): 3737.79, 3554.56, 3446.56, 3002.96, 2925.81, 2839.02, 2732.94, 2609.51, 2325.99, 1836.11, 1743.53, 1641.31, 1548.73, 1461.94, 1326.93, 1259.43, 1124.42, 975.91, 825.48, 769.54 cm^{-1}. LC-MS *m*/*z*: 589.20 $[M+1]^+$.

4.1.16. 2-(4-Chlorophenylsulfonamido)-N-(4-(2-(6,7-dimethoxy-3,4-dihydroisoquinolin-2(1H)-yl)ethyl)phenyl)benzamide (**10**)

The compound was synthesized following general procedure B and D, purified by column chromatography on silica gel (6.3% MeOH/CH_2Cl_2, $R_f = 0.3$). The product was obtained as a light yellow powder (78% yield), mp: 283–285 °C. ^{1}HNMR (400 MHz, CD_3OD): δ(ppm) = 2.95–3.0 (m, 3H, $-CH_2-$), 6.74 (s, 1H, Ar–H), 6.79 (s, 1H, Ar–H), 7.224 (t, 1H, *J* = 8.8 Hz, Ar–H), 7.296–7.317 (m, 3H, *J* = 6.4 Hz, 2 Hz, Ar–H), 7.38–7.40 (d, 2H, *J* = 8.4 Hz, Ar–H), 7.461–7.499 (t, 1H, *J* = 8 Hz, Ar–H), 7.545–7.638 (m, 5H, Ar–H), 7.67 (d, 1H, *J* = 8.0 Hz, Ar–H), 7.755 (d, 1H, *J* = 8.0 Hz, Ar–H). IR ν_{max} (KBr): 3375.2, 3002.96, 2835.16, 2761.87, 2615.29, 2358.78, 2333.71, 1911.33, 1643.24, 1598.88, 1519.80, 1469.66, 1392.51, 1332.72, 1259.43, 1230.50, 1163.00, 1122.49, 1087.78, 1031.85, 1006.77, 827.41, 765.04 cm^{-1}. LC-MS *m*/*z*: 605.18 (100%), 607.17(36.5%).

4.1.17. 2-(4-tert-Butylphenylsulfonamido)-N-(4-(2-(6,7-dimethoxy-3,4-dihydroisoquinolin-2(1H)-yl)ethyl)phenyl) benzamide (**11**)

The compound was synthesized following general procedure B and D, purified by column chromatography on silica gel (6.7% MeOH/CH_2Cl_2, $R_f = 0.45$). The product was obtained as a white powder (87% yield), mp: 139–141 °C. ^{1}HNMR (400 MHz, $CDCl_3$): δ(ppm) = 1.23 (s, 9H, $-CH_3$), 2.77–2.96 (m, 8H, $-CH_2-$), 3.69 (s, 2H, $-N-CH_2-Ar$), 3.866 (s, 3H, Ar–OCH_3), 3.871 (s, 3H, Ar–OCH_3), 6.57 (s, 1H, Ar–H), 6.63 (s, 1H, Ar–H), 7.14 (t, 1H, *J* = 7.6 Hz, Ar–H), 7.27 (d, 2H, *J* = 7.2 Hz, Ar–H), 7.36 (d, 2H, *J* = 8.8 Hz, Ar–H), 7.43 (d, 2H, *J* = 8.0 Hz, Ar–H), 7.47 (d, 1H, *J* = 8.4 Hz, Ar–H), 7.52 (d, 1H, *J* = 7.6 Hz, Ar–H), 7.73 (d, 3H, *J* = 8.8 Hz, Ar–H). IR ν_{max} (KBr): 3446.56, 2960.53, 2378.07, 2312.49, 1645.17, 1598.88, 1515.94, 1463.87, 1330.79, 1259.43, 1230.5, 1122.49, 1081.99, 973.99, 833.19, 757.97 cm^{-1}. ESI-MS (*m*/*z*): 627.20 $[M]^+$.

4.1.18. N-(4-(2-(6,7-Dimethoxy-3,4-dihydroisoquinolin-2(1H)-yl) ethyl)phenyl)-2-(4-fluorophenylsulfonamido)benzamide (**12**)

The compound was synthesized following general procedure B and D, purified by column chromatography on silica gel (12.5% MeOH/CH_2Cl_2, $R_f = 0.36$). The product was obtained as a white powder (87% yield), mp: 148–149 °C. ^{1}HNMR (400 MHz, $CDCl_3$): δ(ppm) = 2.73–2.92 (m, 8H, $-CH_2-$), 3.64 (s, 2H, $-N-CH_2-Ar$), 3.818 (s, 3H, Ar–OCH_3), 3.824 (s, 3H, Ar–OCH_3), 6.52 (s, 1H, Ar–H), 6.58 (s, 1H, Ar–H), 6.96 (t, 2H, *J* = 8.4 Hz, Ar–H), 7.12 (t, 1H, *J* = 7.6 Hz, Ar–H), 7.23 (d, 2H, *J* = 8.0 Hz, Ar–H), 7.37 (d, 2H, *J* = 8.4 Hz, Ar–H), 7.43 (t, 1H, *J* = 8.0 Hz, Ar–H), 7.48 (d, 1H, *J* = 7.6 Hz, Ar–H), 7.66 (d, 1H, *J* = 8.4 Hz, Ar–H), 7.74 (q, 2H, *J* = 8.4 Hz, *J* = 4.8 Hz, Ar–H). IR ν_{max} (KBr): 3438.84, 2925.81, 2848.67, 2387.71, 2308.63, 1643.24, 1596.95, 1517.87, 1463.87, 1328.86, 1259.43, 1230.5, 1163, 1124.42, 1087.78, 975.91, 835.12, 757.97 cm^{-1}. ESI-MS (*m*/*z*): 588.95 $[M]^+$.

4.1.19. 2-(2,5-Dichlorophenylsulfonamido)-N-(4-(2-(6,7-dimethoxy-3,4-dihydroisoquinolin-2(1H)-yl)ethyl)phenyl) benzamide (**13**)

The compound was synthesized following general procedure B and D, purified by column chromatography on silica gel (10% MeOH/$CHCl_3$, $R_f = 0.35$). The product was obtained as a light yellow powder (95% yield), mp: 209–210 °C. ^{1}HNMR (400 MHz, $CDCl_3$): δ(ppm) = 2.73–2.92 (m, 8H, $-CH_2-$), 3.65 (s, 2H, $-N-CH_2-Ar$), 3.822 (s, 3H, Ar–OCH_3), 3.829 (s, 3H, Ar–OCH_3), 6.52 (s, 1H, Ar–H), 6.58 (s, 1H, Ar–H), 7.07 (t, 1H, *J* = 8.0 Hz, Ar–H), 7.21 (d, 2H, *J* = 7.4 Hz, Ar–H), 7.23 (d, 2H, *J* = 7.6 Hz, Ar–H), 7.30 (d, 1H, *J* = 8.8 Hz, Ar–H), 7.35 (d, 1H, *J* = 8.8 Hz, Ar–H), 7.41 (t, 1H, *J* = 8.0 Hz, Ar–H), 7.47 (d, 1H, *J* = 8.8 Hz, Ar–H), 7.50 (d, 1H, *J* = 8.4 Hz, Ar–H), 7.57 (d, 1H, *J* = 8.4 Hz, Ar–H), 8.13 (d, Ar–COH–Ar). IR ν_{max} (KBr): 3855.44, 3739.72, 3676.07, 3616.28, 3442.7, 2921.96, 2852.52, 2356.85, 2320.21, 1743.53, 1647.1, 1515.94, 1460.01, 1334.65, 1259.43, 1122.49, 829.33 cm^{-1}. ESI-MS (*m*/*z*): 637.947 $[M-1]^+$.

4.1.20. N-(4-(2-(6,7-Dimethoxy-3,4-dihydroisoquinolin-2(1H)-yl) ethyl)phenyl)-2-(4-methylphenylsulfonamido)benzamide (**14**)

The compound was synthesized following general procedure B and D, purified by column chromatography on silica gel (6.7% MeOH/CH_2Cl_2, $R_f = 0.34$). The product was obtained as a light yellow powder (92% yield), mp: 121–123 °C. ^{1}HNMR (400 MHz, $CDCl_3$): δ(ppm) = 2.25 (s, 3H, $-CH_3$), 2.79–2.91 (m, 8H, $-CH_2-$), 3.66 (s, 2H, $-N-CH_2-Ar$), 3.814 (s, 3H, $-OCH_3$), 3.820 (s, 3H, $-OCH_3$), 5.27 (s, 1H, –NH–), 6.52 (s, 1H, Ar–H), 6.58 (s, 1H, Ar–H), 7.07–7.10 (m, 3H, Ar–H), 7.22 (d, 2H, *J* = 8.0 Hz, Ar–H), 7.40 (t, 3H, *J* = 8.0 Hz, Ar–H), 7.46 (d, 1H, *J* = 7.6 Hz, Ar–H), 7.61 (d, 2H, *J* = 8.4 Hz, Ar–H), 7.66 (d, 1H, *J* = 7.4 Hz, Ar–H). MS (*m*/*z*): 584.819 $[M]^+$.

4.1.21. N-(4-(2-(6,7-Dimethoxy-3,4-dihydroisoquinolin-2(1H)-yl) ethyl)phenyl)-2-(4-methoxyphenylsulfonamido)benzamide (**15**)

The compound was synthesized following general procedure C and D, purified by column chromatography on silica gel (7.1% MeOH/CH_2Cl_2, $R_f = 0.4$). The product was obtained as a light yellow powder (90% yield), mp: 118–120 °C. ^{1}HNMR (400 MHz, $CDCl_3$): δ(ppm) = 2.74–2.93 (m, 8H, $-CH_2-$), 3.655 (s, 2H, $-N-CH_2-Ar$), 3.667 (s, 3H, Ar–OCH_3), 3.818 (s, 3H, Ar–OCH_3), 3.825 (s, 3H, Ar–OCH_3), 5.28 (s, 1H, $-SO_2-NH-$), 6.52 (s, 1H, Ar–H), 6.58 (s, 1H,

Ar–H), 6.72 (d, 2H, J = 8.8 Hz, Ar–H), 7.105 (t, 1H, J = 7.2 Hz, Ar–H), 7.22 (d, 2H, J = 8.0 Hz, Ar–H), 7.383 (d, 2H, J = 8.0 Hz, Ar–H), 7.42 (d, 1H, J = 8.4 Hz, Ar–H), 7.45 (d, 1H, J = 8.0 Hz, Ar–H), 7.64 (s, 1H, –CONH–), 7.66 (d, 3H, J = 8.4 Hz, Ar–H). IR ν_{max} (KBr): 3442.7, 2927.74, 1645.17, 1598.88, 1515.94, 1463.87, 1330.79, 1257.5, 1157.21, 1122.49, 1020.27, 831.26 cm^{-1}. ESI-MS (m/z): 600.792 $[M-1]^+$.

4.1.22. 2-(4-tert-Butylphenylsulfonamido)-N-(4-(2-(6,7-dimethoxy-3,4-dihydroisoquinolin-2(1H)-yl)ethyl)phenyl)-4,5-dimethoxybenzamide (**16**)

Starting from 6-Nitroveratric acid, the compound was synthesized following general procedure C and D, purified by column chromatography on silica gel (10% MeOH/CH_2Cl_2, R_f = 0.3). The product was obtained as a light yellow powder (87% yield), mp: 153–155 °C. ^{1}HNMR (400 MHz, $CDCl_3$): δ(ppm) = 1.18 (s, 9H, $-C(CH_3)_3$), 2.75–2.92 (m, 8H, $-CH_2-$), 3.68 (s, 2H, $-N-CH_2-Ar$), 3.82 (s, 6H, Ar–OCH_3), 3.845 (s, 3H, Ar–OCH_3), 3.851 (s, 3H, Ar–OCH_3), 6.52 (s, 1H, Ar–H), 6.57 (s, 1H, Ar–H), 6.90 (s, 1H, Ar–H), 7.14 (s, 1H, Ar–H), 7.18 (d, 2H, J = 8.4 Hz, Ar–H), 7.30 (d, 2H, J = 8.8 Hz, Ar–H), 7.36 (d, 2H, J = 8.0 Hz, Ar–H), 7.63 (d, 2H, J = 8.4 Hz, Ar–H). ESI-MS (m/z): 687.495 $[M]^+$.

4.1.23. N-(4-(2-(6,7-Dimethoxy-3,4-dihydroisoquinolin-2(1H)-yl)ethyl)phenyl)-4,5-dimethoxy-2-(4-(trifluoromethyl)phenylsulfonamido)benzamide (**17**)

Starting from 6-Nitroveratric acid, the compound was synthesized following general procedure C and D, purified by column chromatography on silica gel (10% MeOH/CH_2Cl_2, R_f = 0.35). The product was obtained as a light yellow powder (89% yield), mp: 161–163 °C. ^{1}HNMR (400 MHz, $CDCl_3$): δ(ppm) = 2.77–2.93 (m, 8H, $-CH_2-$), 3.69 (s, 2H, $-N-CH_2-Ar$), 3.82 (s, 6H, Ar–OCH_3), 3.85 (s, 3H, Ar–OCH_3), 3.89 (s, 3H, Ar–OCH_3), 5.28 (s, 1H, $-SO_2NH-Ar$), 6.52 (s, 1H, Ar–H), 6.57 (s, 1H, Ar–H), 6.87 (s, 1H, Ar–H), 7.18 (d, 2H, J = 7.6 Hz, Ar–H), 7.21 (s, 1H, Ar–H), 7.29 (d, 2H, J = 7.6 Hz, Ar–H), 7.79 (d, 2H, J = 8.4 Hz, Ar–H).

4.1.24. N-(4-(2-(6,7-Dimethoxy-3,4-dihydroisoquinolin-2(1H)-yl)ethyl)phenyl)-4,5-dimethoxy-2-(4-methylphenylsulfonamido)benzamide (**18**)

Starting from 6-Nitroveratric acid, the compound was synthesized following general procedure C and D, purified by column chromatography on silica gel (10% MeOH/CH_2Cl_2, R_f = 0.3). The product was obtained as a light yellow powder (88% yield), mp: 171–173 °C. ^{1}HNMR (400 MHz, $CDCl_3$): δ(ppm) = 2.25 (s, 3H, Ar–CH_3), 2.28–2.94 (m, 8H, $-CH_2-$), 3.70 (s, 2H, $-N-CH_2-Ar$), 3.821 (s, 3H, $-Ar-OCH_3$), 3.828 (s, 3H, Ar–OCH_3), 3.838 (s, 3H, Ar–OCH_3), 3.888 (s, 3H, Ar–OCH_3), 6.52 (s, 1H, Ar–H), 6.58 (s, 1H, Ar–H), 6.86 (s, 1H, Ar–H), 7.04 (d, 2H, J = 8.4 Hz, Ar–H), 7.20 (s, 1H, Ar–H), 7.22 (d, 2H, J = 7.6 Hz, Ar–H), 7.34 (d, 2H, J = 7.6 Hz, Ar–H), 7.56 (d, 2H, J = 8.4 Hz, Ar–H).

4.1.25. (9H-Fluoren-9-yl)methyl 2-(4-(2-(6,7-dimethoxy-3,4-dihydroisoquinolin-2(1H)-yl)ethyl)phenylcarbamoyl)phenylcarbamate (**19**)

The compound was synthesized following general procedure B and E, purified by column chromatography on silica gel (4% MeOH/CH_2Cl_2, R_f = 0.5). The product was obtained as a yellow powder (76% yield), mp: 124–125 °C. ^{1}HNMR (400 MHz, $CDCl_3$): δ(ppm) = 2.8–3.5 (m, 8H, $-CH_2-$), 3.78 (s, 3H, Ar–OCH_3), 3.80 (s, 3H, Ar–OCH_3), 3.90 (s, 2H, $-N-CH_2-Ar$), 4.22 (s, 1H, $-CH=$), 4.37 (s, 2H, $-CH_2-O-$), 6.45 (s, 1H, Ar–H), 6.55 (s, 1H, Ar–H), 7.03 (s, 1H, Ar–H), 7.10 (d, 1H, J = 8.0 Hz, Ar–H), 7.34–7.40 (m, 4H, Ar–H), 7.54–7.60 (m, 5H, Ar–H), 7.71 (d, 4H, J = 8.0 Hz, Ar–H), 8.25 (s, 1H, Ar–H), 8.87 (s, 1H, –NH–), 10.50 (s, 1H, –NH–CO–). IR ν_{max} (KBr): 3988.52, 3743.57, 3446.56, 2925.81, 2852.52, 2335.64, 1730.03, 1649.02, 1593.09, 1517.87, 1448.44, 1409.87, 1367.44, 1326.93, 1261.36, 1215.07, 1118.64, 1043.42, 908.41 cm^{-1}. LC-MS (m/z): 652.29 $[M-1]^+$.

4.1.26. N-(4-(2-(6,7-Dimethoxy-3,4-dihydroisoquinolin-2(1H)-yl)ethyl)phenyl)-2-dodecanamidobenzamide (**20**)

The compound was synthesized following general procedure B and E, purified by column chromatography on silica gel (5% MeOH/CH_2Cl_2, R_f = 0.5). The product was obtained as a light yellow powder (87% yield), mp: 145–147 °C. ^{1}HNMR (400 MHz, $CDCl_3$): δ(ppm) = 0.87 (t, 3H, J = 6.6 Hz, $-CH_2-CH_3$), 1.25–1.4 (m, 16H, $-CH_2-CH_2-$), 1.71 (t, 2H, J = 8.0 Hz, $-CH_2-$), 2.35 (t, 2H, J = 8.0 Hz, $-CH_2-O-$), 2.09 (s, 3H, $-COCH_3$), 2.76–2.95 (m, 8H, $-CH_2-$), 3.66 (s, 2H, $-N-CH_2-Ar$), 3.84 (s, 6H, Ar–OCH_3), 6.55 (s, 1H, Ar–H), 6.61 (s, 1H, Ar–H), 7.03 (t, 1H, J = 8.0 Hz, Ar–H), 7.28 (d, 1H, J = 8.0 Hz, Ar–H), 7.37 (t, 1H, J = 8.0 Hz, Ar–H), 7.54 (d, 1H, J = 8.0 Hz, Ar–H),7.58 (d, 2H, J = 8.0 Hz, Ar–H), 8.44 (d, 1H, J = 7.6 Hz), 8.47–8.51 (m, 1H, Ar–H), 10.64 (s, 1H, –NH–). IR ν_{max} (KBr): 3894.01, 3743.57, 3620.14, 3278.76, 2921.96, 2850.59, 2364.57, 2322.13, 1658.67, 1596.95, 1515.94, 1446.51, 1409.87, 1323.08, 1257.5, 1130.21, 1014.49, 825.48 cm^{-1}. LC-MS (m/z): 612.5 $[M-1]^+$.

4.1.27. 2-Cinnamamido-N-(4-(2-(6,7-dimethoxy-3,4-dihydroisoquinolin-2(1H)-yl)ethyl)phenyl)benzamide (**21**)

The compound was synthesized following general procedure B and E, purified by column chromatography on silica gel (10% MeOH/CH_2Cl_2, R_f = 0.5). The product was obtained as a light yellow powder (84% yield), mp: 94–95 °C. ^{1}HNMR (400 MHz, $CDCl_3$): δ(ppm) = 2.74–2.93 (m, 8H, $-CH_2-$), 3.64 (s, 2H, $-N-CH_2-Ar$), 3.82 (s, 3H, Ar–OCH_3), 3.83 (s, 3H, Ar–OCH_3), 6.53 (s, 1H, Ar–H), 6.56 (d, 1H, J = 16 Hz, $-CH=CH-$), 6.59 (s, 1H, Ar–H), 7.08 (t, 1H, J = 8.0 Hz, Ar–H), 7.28 (d, 2H, J = 8.0 Hz, Ar–H), 7.36 (s, 1H, Ar–H), 7.37 (d, 2H, J = 8.0 Hz, Ar–H), 7.47 (t, 1H, J = 7.6 Hz, Ar–H), 7.54–7.59 (m, 4H, Ar–H), 7.71 (s, 1H, Ar–H), 7.75 (s, 1H, –CO–NH–), 8.18–8.21 (m, 1H, Ar–H), 8.68 (d, 1H, J = 8.4 Hz, Ar–H), 11.0 (s, 1H, –NH–). IR ν_{max} (KBr): 3448.49, 3263.33, 2933.53, 2825.25, 1685.67, 1679.88, 1625.88, 1595.02, 1525.59, 1458.17, 1263.29, 966.27 cm^{-1}. ESI-MS (m/z): 560.517 $[M-1]^+$.

4.1.28. N-(2-(4-(2-(6,7-Dimethoxy-3,4-dihydroisoquinolin-2(1H)-yl)ethyl)phenylcarbamoyl)phenyl)-4-fluoro-2-nitrobenzamide (**22**)

The compound was synthesized following general procedure B and E, purified by column chromatography on silica gel (6.7% MeOH/CH_2Cl_2, R_f = 0.4). The product was obtained as a yellow powder (80% yield), mp: 192–194 °C. ^{1}HNMR (400 MHz, $CDCl_3$): δ(ppm) = 2.74–2.91 (m, 8H, $-CH_2-$), 3.64 (s, 2H, $-N-CH_2-Ar$), 3.83 (s, 3H, Ar–OCH_3), 3.84 (s, 3H, Ar–OCH_3), 6.53 (s, 1H, Ar–H), 6.60 (s, 1H, Ar–H), 7.23 (t, 1H, J = 5.2 Hz, Ar–H), 7.25 (s, 1H, Ar–H), 7.39–7.42 (m, 1H, Ar–H), 7.44 (s, 1H, Ar–H), 7.45 (s, 1H, Ar–H), 7.52–7.53 (m, 1H, Ar–H), 7.58 (t, 1H, J = 4.8 Hz, Ar–H), 7.69 (t, 1H, J = 4.0 Hz, Ar–H), 7.70–7.72 (m, 1H, Ar–H), 7.75 (dd, 1H, J = 2.0 Hz, 6.0 Hz), 8.02 (s, 1H, –NH–), 8.70 (d, 1H, J = 1.6 Hz), 11.45 (s, 1H, –NH–). IR ν_{max} (KBr): 3739.72, 3577.71, 3350.12, 3209.33, 3066.61, 2954.74, 2927.74, 2823.59, 2748.37, 2316.35, 1731.96, 1679.88, 1662.52, 1515.94, 1448.44, 1353.94, 1311.5, 1253.64, 1016.42, 939.27, 767.62 cm^{-1}. ESI-MS (m/z): 597.47 $[M-1]^+$.

4.1.29. N-(2-(4-(2-(6,7-Dimethoxy-3,4-dihydroisoquinolin-2(1H)-yl)ethyl)phenylcarbamoyl)phenyl)furan-2-carboxamide (**23**)

The compound was synthesized following general procedure B and E, purified by column chromatography on silica gel (10% MeOH/CH_2Cl_2, R_f = 0.4). The product was obtained as a light yellow powder (82% yield), mp: 170–172 °C. ^{1}HNMR (400 MHz, $CDCl_3$): δ(ppm) = 2.73–2.98 (m, 8H, $-CH_2-$), 3.64 (s, 2H, $-N-CH_2-Ar$), 3.82 (s, 3H, Ar–OCH_3), 3.83 (s, 3H, Ar–OCH_3), 6.51–6.52 (m, 1H,

Ar–H), 6.53 (s, 1H, Ar–H), 6.60 (s, 1H, Ar–H), 7.06 (t, 1H, J = 6.8 Hz, Ar–H), 7.21 (d, 1H, J = 4.0 Hz, Ar–H), 7.27 (d, 2H, J = 8.0 Hz, Ar–H), 7.47 (t, 1H, J = 8.0 Hz, Ar–H), 7.55 (d, 3H, J = 8.0 Hz, Ar–H), 7.60 (d, 1H, J = 8.0 Hz, Ar–H), 8.11 (s, 1H, –NH–), 8.59–8.66 (dd, 1H, J = 4.0 Hz, J = 20.0 Hz, Ar–H), 11.63 (s, 1H, –NH–). IR ν_{max} (KBr): 3510.2, 3276.83, 3130.25, 2966.31, 2835.16, 2765.73, 2385.78, 1855.39, 1643.24, 1606.59, 1593.09, 1517.87, 1446.51, 1413.72, 1367.44, 1321.15, 1261.36, 1228.57, 1126.35, 1010.63, 877.55, 823.55 cm^{-1}. ESI-MS (m/z): 524.03 $[M-1]^+$.

4.1.30. N-(2-(4-(2-(6,7-Dimethoxy-3,4-dihydroisoquinolin-2(1H)-yl)ethyl)phenylcarbamoyl)phenyl)quinoline-3-carboxamide (**24**)

The compound was synthesized following general procedure B and E, purified by column chromatography on silica gel (10% MeOH/CH_2Cl_2, R_f = 0.35). The product was obtained as a light yellow powder (80% yield), mp: 197–199 °C. ^{1}HNMR (400 MHz, $CDCl_3$): δ(ppm) = 2.79–3.00 (m, 8H, $-CH_2-$), 3.68 (s, 2H, $-N-CH_2-Ar$), 3.83 (s, 6H, $Ar-OCH_3$), 6.52 (s, 1H, Ar–H), 6.59 (s, 1H, Ar–H), 7.14 (t, 1H, J = 7.6 Hz, Ar–H), 7.27 (d, 2H, J = 8.4 Hz, Ar–H), 7.55 (t, 1H, J = 8.0 Hz, Ar–H), 7.58 (d, 2H, J = 8.4 Hz, Ar–H), 7.63 (t, 1H, J = 7.6 Hz, Ar–H), 7.68 (d, 1H, J = 7.6 Hz, Ar–H), 7.82 (t, 1H, J = 7.6 Hz, Ar–H), 7.99 (d, 1H, J = 8.4 Hz, Ar–H), 8.16 (d, 1H, J = 8.4 Hz, Ar–H), 8.19 (s, 1H, Ar–NHCO–), 8.77 (s, 1H, Ar–H), 8.78 (d, 2H, J = 8.0 Hz, Ar–H), 9.52 (d, 1H, J = 2.0 Hz, Ar–H), 12.22 (s, 1H, Ar–NHCO–). MS (m/z): 585.495.

4.1.31. N-(2-(4-(2-(6,7-Dimethoxy-3,4-dihydroisoquinolin-2(1H)-yl)ethyl)phenylcarbamoyl)-4,5-dimethoxyphenyl)quinoline-3-carboxamide (**25**) (tariquidar, XR9576)

Starting from 6-Nitroveratric acid, the compound was synthesized following general procedure C and E, purified by column chromatography on silica gel (10% MeOH/CH_2Cl_2, R_f = 0.36). The product was obtained as a light brown powder (75% yield), mp: 133–135 °C. ^{1}HNMR (400 MHz, $CDCl_3$): δ(ppm) = 2.66–2.79 (m, 8H, $-CH_2-$), 3.52 (s, 2H, $-NCH_2-Ar$), 3.674 (s, 3H, Ar–OMe), 3.678 (s, 3H, Ar–OMe), 3.87 (s, 6H, Ar–OMe), 6.62 (d, 2H, J = 8.4 Hz, Ar–H), 7.24 (d, 2H, J = 7.6 Hz, Ar–H), 7.50 (s, 1H, Ar–H), 7.57 (d, 2H, J = 8.0 Hz, Ar–H), 7.71 (t, 1H, J = 7.6 Hz, Ar–H), 7.90 (t, 1H, J = 7.2 Hz, Ar–H), 8.09 (d, 1H, J = 8.4 Hz, Ar–H), 8.13 (d, 1H, J = 8.4 Hz, Ar–H), 8.24 (s, 1H, Ar–H), 8.87 (s, 1H, Ar–H), 9.33 (s, 1H, Ar–H), 10.34 (s, 1H, –CONH–Ar), 12.28 (s, 1H, –CONH–Ar). MS (m/z): 645.226 $[M^+]$.

4.2. Biology

4.2.1. Materials

Doxorubicin hydrochloride was purchased from Enzo (New York, NY, USA). Verapamil was obtained from Sigma–Aldrich (St Louis, MO, USA). Pheophorbide A (PhA), fumitremorgin C (FTC), MK571 and PSC833 were kind gifts provided by Dr Susan Bates (National Cancer Institute, NIH, Bethesda, MD). Phycoerythrin (PE)-conjugated anti-P-gp antibody UIC2, PE-conjugated anti-BCRP antibody 5D3 or PE-conjugated mouse IgG2b negative control antibody were obtained from eBioscience Inc (San Diego, CA). All other reagents were from Sigma–Aldrich.

4.2.2. Cell culture

HCT116 and CCD18-Co cells were purchased from ATCC. HCT116 cells were cultured in RPMI1640 medium. CCD18-Co cells were cultured in EMEM medium with 10% FBS, 100 units/mL streptomycin sulfate and 100 units/mL penicillin G sulfate. The following cell lines are generous gift provided by Dr Susan Bates (National Cancer Institute, USA): (1) parental K562 human leukemia cells and its P-gp or BCRP-stable transfected cell lines; (2) pcDNA3 or MRP1-stable transfected HEK293 cells; (3) parental MCF-7 human breast cancer cell line and its drug-selected BCRP-overexpressing MCF-7 FLV1000 subline; (4) parental SW620 human colon cancer cell line and it doxorubicin-selected P-gp-overexpressing SW620 Ad300 subline. LCC6 and its P-gp-overexpressing subline LCC6 MDR are provided by Prof. Robert Clarke (Georgetown University, Washington DC, U.S.A). The cells have been fully characterized and proven to be useful models for studying multidrug resistant transporters-mediated resistance and their reversal. These cell lines were maintained either in DMEM or RPMI1640 medium supplemented with 10% fetal bovine serum, 100 units/mL streptomycin sulfate, and 100 units/mL penicillin G sulfate, and 2 mg/mL G418, and incubated at 37 °C in 5% CO_2.

4.2.3. MTT assay for the cytotoxicity and the SRB assay for growth inhibition

Drug cytotoxicity or cancer cell growth inhibition was performed by the MTT or SRB assay. Briefly, cells were seeded in 96-well plates and cultured for 24 h before treatment. The compounds were dissolved in DMSO. A series of concentrations of the compounds were added into the cells and cultured for another 24 h, 48 h or 72 h. Cell viability was detected 4 h after adding of MTT. The growth inhibitory effect of individual anticancer drugs was evaluated by the sulforhodamine B assay as described previously [28]. The IC_{50} values of each agent were subsequently determined by Prism 4.0 (Graphpad Software). For the combination drug treatment, drugs were given simultaneously for 72 h for the evaluation of combination cytotoxic effects.

4.2.4. Drug combination

Cells were seeded in 96-well plates and cultured for 24 h before treatment. The compounds were dissolved in DMSO. The cells were pretreated with tariquidar derivatives (1 μM) for 1 h before treated with doxorubicin (0–100 μM) and cultured for another 48 h. Cell viability was detected after adding of MTT for 4 h.

4.2.5. Flow cytometry-based substrate efflux assay

A flow cytometry-based assay was employed to study the possible efflux inhibition of the three major ABC transporters by the tested tariquidar derivatives as described previously with minor modification [29]. Briefly, cells were trypsinized and incubated for 30 min in phenol red-free complete medium with the desired fluorescent substrate (10 μM doxorubicin, 0.5 mg/mL rhodamine 123, 1 μM pheophorbide A, or 0.2 μM calcein AM) in the presence or absence of the tested tariquidar derivatives. Subsequently, the cells were washed twice with ice-cold PBS and incubated in substrate-free medium for 1 h at 37 °C continuing with the tested inhibitors to generate the inhibitor/efflux histogram, or without the inhibitor to generate the efflux histogram. Tariquidar or verapamil served as positive control. The inhibited efflux was determined as the difference in mean fluorescence intensity (MFI) between the inhibitor/efflux and efflux histograms. To determine significant difference between intracellular fluorescence values, the Student's t-test was performed with $p < 0.05$ being considered significant. Cells were finally washed with cold Dulbecco's PBS and placed on ice in the dark until analysis by flow cytometry. Inhibitors specific for P-gp, BCRP and MRP1 (i.e. PSC833, FTC and MK571, respectively) were used as control for comparison. Tariquidar derivatives with transporter inhibitory effect will shift the inhibitor/efflux histogram to the right, indicating retention of the fluorescent substrate in the cells. Samples were analyzed on a LSRFortessa Cell Analyzer (BD Biosciences, San Jose, CA). Rhodamine/calcein AM fluorescence was detected with a 488-nm argon laser and a 530-nm bandpass-filter whereas PhA fluorescence was detected with a 488-nm argon laser and a 670-nm bandpass filter. At least 10,000 events were collected for all flow cytometry studies. Cell debris was

eliminated by gating on forward versus side scatter and dead cells were excluded based on propidium iodide staining. All assays were performed in three independent experiments.

4.2.6. UIC2 or 5D3 shift assay for assessing interaction between tariquidar derivatives and P-gp or BCRP

The binding of the conformational sensitive UIC2 or 5D3 antibody to intact cells (K562/P-gp or K562/BCRP) in the presence or absence of the tested tariquidar derivatives was measured by flow cytometer as described previously [26]. Cells were pre-incubated with the tested compounds in 0.5% bovine serum albumin/Dulbecco's PBS for 10 min at 37 °C before labeling with 0.5 g/mL of PE-conjugated anti-P-gp antibody UIC2, PE-conjugated anti-BCRP antibody 5D3 or PE-conjugated mouse IgG2b negative control antibody for another 45 min at 37 °C. The tested compounds were present during the antibody labeling. As positive control for maximum labeling, UIC2 and 5D3 binding was determined in the presence of 1 M PSC833 (specific P-gp inhibitor) and 5 M FTC (specific BCRP inhibitor), respectively.

4.2.7. ATPase assay

A colorimetric ATPase assay was performed as previously described with minor modification [30]. Briefly, crude membranes isolated from High Five insect cells expressing either P-gp or BCRP (100 μg protein/mL) were incubated at 37 °C with a range of different concentrations of the tested tariquidar derivatives in the presence or absence of sodium orthovanadate (0.3 μM for P-gp and 1.2 μM for BCRP) in ATPase assay buffer (50 mM KCl, 5 mM sodium azide, 2 mM EDTA, 10 mM $MgCl_2$, 1 mM DTT, pH 6.8) for 5 min. The crude membranes were kind gift provided by Dr. Suresh Ambudkar (National Cancer Institute, NIH, USA). ATP hydrolysis reaction was then started by the addition of 5 mM Mg-ATP (concentration in a final volume of 60 μL) and incubated for 20 min (for P-gp) or 10 min (for BCRP). SDS solution (30 μL of 10% SDS) was then added to terminate the reaction. After the addition of a detection reagent (35 mM ammonium molybdate, 15 mM zinc acetate, 10% ascorbic acid) and incubation at 37 °C for 20 min, absorbance was measured at 750 nm. The amount of inorganic phosphate released was estimated by reading from a standard curve. Specific modulation of P-gp and BCRP ATPase activity (i.e. vanadate-sensitive) was determined as the difference between the amounts of inorganic phosphate released from ATP in the absence and presence of sodium orthovanadate.

Statement of interest

The authors declare no competing financial interest.

Acknowledgements

This work is in memory of Prof. H.K. Yeung from The Chinese University of Hong Kong for his great support. This research was financially supported by Beijing Science Nova Program (No. 2008B20) and Fundamental Research Funds for the Central Universities (No. FRF-BR-14-002A).

Appendix A. Supplementary data

Supplementary data related to this article can be found at http://dx.doi.org/10.1016/j.ejmech.2015.06.049.

References

[1] D.B. Longley, P.G. Johnston, Molecular mechanisms of drug resistance, J. Pathol. 205 (2005) 275–292.
[2] G. Szakacs, J.K. Paterson, J.A. Ludwig, C. Booth-Genthe, M.M. Gottesman, Targeting multidrug resistance in cancer, Nat. Rev. Drug Discov. 5 (2006) 219–234.
[3] T. Tsuruo, H. Iida, S. Tsukagoshi, Y. Sakurai, Overcoming of vincristine resistance in P388 leukemia in vivo and in vitro through enhanced cytotoxicity of vincristine and vinblastine by verapamil, Cancer Res. 41 (1981) 1967–1972.
[4] G.D. Leonard, T. Fojo, S.E. Bates, The role of ABC transporters in clinical practice, Oncologist 8 (2003) 411–424.
[5] L. Pusztai, P. Wagner, N. Ibrahim, E. Rivera, R. Theriault, D. Booser, Phase II study of tariquidar, a selective P-glycoprotein inhibitor, in patients with chemotherapy-resistant, advanced breast carcinoma, Cancer 104 (4) (2005) 682–691.
[6] H. Ryder, P.A. Ashworth, M.J. Roe, J. Brumwell, S. Hunjan, A. Folkes, J. Sanderson, Anthranilic Acid Derivatives as Multi Drug Resistance Modulators, WO98/17648, April 30, 1998.
[7] M. Roe, A. Folkes, P. Ashworth, J. Brumwell, L. Chima, S. Hunjan, I. Pretswell, W. Dangerfield, H. Ryder, P. Charlton, Reversal of P-glycoprotein mediated multidrug resistance by novel anthranilamide derivatives, Bioorg. Med. Chem. Lett. 9 (1999) 595–600.
[8] C. Martin, G. Berridge, P. Mistry, C. Higgins, P. Charlton, R. Callaghan, The molecular interaction of the high affinity reversal agent XR9576 with P-glycoprotein, Br. J. Pharmacol. 128 (1999) 403–411.
[9] M.M. Malingre, J.H. Beijnen, H. Rosing, F.J. Koopman, R.C. Jewell, E.M. Paul, et al., Co-administration of GF120918 significantly increases the systemic exposure to oral paclitaxel in cancer patients, Br. J. Cancer 84 (2001) 42–47.
[10] P. Mistry, A.J. Stewart, W. Dangerfield, S. Okiji, C. Liddle, D. Bootle, J.A. Plumb, D. Templeton, P. Charlton, In vitro and in vivo reversal of P-glycoprotein-mediated multidrug resistance by a novel potent modulator, XR9576, Cancer Res. 61 (2001) 749–758.
[11] J. Walker, C. Martin, R. Callaghan, Inhibition of P-glycoprotein function by XR9576 in a solid tumour model can restore anticancer drug efficacy, Eur. J. Cancer 40 (2004) 594–605.
[12] S. Nobili, I. Landini, B. Giglioni, E. Mini, Pharmacological strategies for overcoming multidrug resistance, Curr. Drug Targets 7 (7) (2006) 861–879.
[13] K.P. Ilza, M. Wiese, Structure-activity relationships of tariquidar analogs as multidrug resistance modulators, AAPS J. 11 (3) (2009) 435–444.
[14] R.J. Kelly, D. Draper, C.C. Chen, R.W. Robey, W.D. Figg, R.L. Piekarz, X. Chen, E.R. Gardner, F.M. Balis, A.M. Venkatesan, S.M. Steinberg, T. Fojo, S.E. Bates, A pharmacodynamic study of docetaxel in combination with the p-glycoprotein antagonist tariquidar (XR9576) in patients with lung, ovarian, and cervical Cancer, Clin. Cancer Res. 17 (3) (2011) 569–580.
[15] (a) I.K. Pajeva, C. Globisch, M. Wiese, Structure-function relationships of multidrug resistance P-glycoprotein, J. Med. Chem. 47 (2004) 2523–2533;
(b) C. Globisch, I.K. Pajeva, M. Wiese, Bioorg. Med. Chem. 14 (2006) 1588–1598.
[16] (a) E. Michael, L. Xuqin, M. Christine, B. Gunther, B. Armin, K. Burkhard, Tariquidar analogues: synthesis by CuI-catalysed N/O-aryl coupling and inhibitory activity against the ABCB1 transporter, Eur. J. Org. Chem. 16 (2007) 2643–2649;
(b) A.C. Nicola, B. Francesco, C. Mariangela, G.P. Maria, C. Marialessandra, I. Carmela, N. Mauro, P. Roberto, A. Amalia, M.S. Grazia, P. Letizia, P. Angelo, Bioorg. Med. Chem. 16 (2008) 362–373;
(c) K. Matthias, E. Michael, M. Christine, M. Anne, B. Gunther, F. Gert, K. Burkhard, B. Armin, J. Med. Chem. 52 (2009) 1190–1197.
[17] V. Jekerle, W. Klinkhammer, R.M. Reilly, M. Piquette-Miller, M. Wiese, Novel tetrahydroisoquinolin-ethyl-phenylamine based multidrug resistance inhibitors with broad-spectrum modulating properties, Cancer Chemother. Pharmacol. 59 (2007) 61–69.
[18] H. Müller, I.K. Pajeva, C. Globisch, M. Wiese, Functional assay and structure-activity relationships of new third-generation P-glycoprotein inhibitors, Bioorg. Med. Chem. 16 (2008) 2448–2462.
[19] H. Müller, W. Klinkhammer, C. Globisch, M.U. Kassack, I.K. Pajeva, M. Wiese, New functional assay of P-glycoprotein activity using Hoechst 33342, Bioorg. Med. Chem. 15 (2007) 7470–7479.
[20] V. Jekerle, W. Klinkhammer, D.A. Scollard, K. Breitbach, R.M. Reilly, M. Piquette-Miller, et al., In vitro and in vivo evaluation of WK-X-34, a novel inhibitor of P-glycoprotein and BCRP, using radio imaging techniques, Int. J. Cancer. 119 (2006) 414–422.
[21] P. Labrie, S.P. Maddaford, S. Fortin, S. Rakhit, L.P. Kotra, R.C. Gaudreault, A comparative molecular field analysis (CoMFA) and comparative molecular similarity indices analysis (CoMSIA) of anthranilamide derivatives that are multidrug resistance modulators, J. Med. Chem. 49 (2006) 7646–7660.
[22] W. Klinkhammer, H. Müller, C. Globisch, I.K. Pajeva, M. Wiese, Synthesis and biological evaluation of a small molecule library of 3rd generation multidrug resistance modulators, Bioorg. Med. Chem. 17 (2009) 2524–2535.
[23] (a) P. Labrie, S.P. Maddaford, J. Lacroix, et al., In vitro activity of novel dual action MDR anthranilamide modulators with inhibitory activity at CYP-450, Bioorg. Med. Chem. 14 (2006) 7972–7987;
(b) P. Labrie, S.P. Maddaford, J. Lacroix, et al., In vitro activity of novel dual action MDR anthranilamide modulators with inhibitory activity on CYP-450 (part 2), Bioorg. Med. Chem. 15 (2007) 3854–3868.
[24] (a) R.B. Wang, C.L. Kuo, L.L. Lien, E.J. Lien, Structure-activity relationship: analyses of p-glycoprotein substrates and inhibitors, J. Clin. Pharm. Ther. 28 (3) (2003) 203–228;
(b) A. Palmeira, E. Sousa, M.H. Vasconcelosand, M.M. Pinto, Three decades of

P-gp inhibitors: skimming through several generations and scaffolds, Curr. Med. Chem. 19 (2012) 1946–2025.
[25] H. Nagy, K. Goda, F. Fenyvesi, Z. Bacso, M. Szilasi, J. Kappelmayer, G. Lustyik, M. Cianfriglia, G.J. Szabo, Distinct groups of multidrug resistance modulating agents are distinguished by competition of P-glycoprotein-specific antibodies, Biochem. Biophys. Res. Commun. 315 (2004) 942–949.
[26] L. Ozvegy, G. Varady, G. Koblos, O. Ujhelly, J. Cervenak, J.D. Schuetz, B.P. Sorrentino, G.J. Koomen, A. Varadi, K. Nemet, B. Sarkadi, Function-dependent conformational changes of the ABCG2 multidrug transporter modify its interaction with a monoclonal antibody on the cell surface, J. Biol. Chem. 280 (2005) 4219–4227.
[27] P. Kannan, S. Telu, S. Shukla, S.V. Ambudkar, V.W. Pike, C. Halldin, M.M. Gottesman, R.B. Innis, M.D. Hall, The "specific" P-glycoprotein inhibitor tariquidar is also a substrate and an inhibitor for breast cancer resistance protein (BCRP/ABCG2), ACS Chem. Neurosci. 2 (2011) 82–89.
[28] P. Skehan, R. Stornet, D. Scudiero, A. Monks, J. McMahon, D. Vistica, J.T. Warren, H. Bokesch, S. Kenney, M.R. Boyd, New colorimetric cytotoxicity assay for anticancer-drug screening, J. Natl. Cancer Inst. 82 (1990) 1107–1112.
[29] K.K. To, S.X. Ren, C.C. Wong, C.H. Cho, Reversal of ABCG2-mediated multidrug resistance by human cathelicidin and its analogs in cancer cells, Peptides 40 (2013) 13–21.
[30] F. Wang, Y.J. Mi, X.G. Chen, X.P. Wu, Z. Liu, S.P. Chen, Y.J. Liang, C. Cheng, K.K. To, L.W. Fu, Axitinib targeted cancer stemlike cells to enhance efficacy of chemotherapeutic drugs via inhibiting the drug transport function of ABCG2, Mol. Med. 18 (2012) 887–898.